**ABSTRACT**

A consortium of six research universities, New Jersey Institute of Technology (NJIT), University of Maryland (UMd), University of New Hampshire (UNH), California Institute of Technology (Caltech), University of Alabama in Huntsville (UAH), and University of Michigan (UMich), plus two industrial laboratories (Bell Laboratories/Lucent Technologies and Raytheon), a federally funded research and development corporation (The Aerospace Corporation) and two government laboratories (Naval Research Laboratory and Air Force Research Laboratory), are proposing a comprehensive, integrated singular suite of solar-terrestrial measurements and modeling that will significantly advance the state of knowledge of, and ability to predict the breadth and impact of space weather. Space weather, as defined in the FY 2001 MURI Topic #29, can significantly, and negatively, impact Department of Defense (DoD) and other space operations as well as military and civilian telecommunication facilities and electric power grids. Our team has unique, dedicated observational capabilities incorporating NJIT's extensive optical and radio observing facilities at Big Bear Solar Observatory (BBSO) and the Solar Array at Owens Valley Radio Observatory (OVSA). We propose to extend our ground-based observations of the sun to 24-hour coverage in two key areas – microwave radio spectroscopy and optical vector magnetography – with world-wide networks ideal for space weather studies. These extensions will be built on our experience in setting up our already operating networks for the study of space weather. Our observational resources will be combined with measurements from additional instruments (associated with consortium members and other groups) located in the heliosphere and within the earth's magnetosphere. For in situ and remote heliospheric observations, we rely on spacecraft data from current missions, SOHO, Wind, Ulysses, and ACE in the interplanetary medium, and Polar, SAMPEX, GOES and national security spacecraft in the magnetosphere. Data from future missions such as Stereo will also be used. The geoeffectiveness of solar events will also be tested based on a number of ground-based geomagnetic monitoring stations. The data to be acquired will be analyzed, synthesized, and modeled by consortium members who are highly experienced space plasma theorists and experimentalists. The central theme of our proposal is to use ground-based solar data together with space-based solar data to understand and forecast the initiation of space weather events, follow their propagadion and development in the heliosphere, and predict their likely impact on the near-earth envyronment. In situ heliospheric and magnetospheric measurements will provide "ground truth" for our work based upon remote sensing techniques.

Using the expertise of our team, we propose to focus on: (1) the 3-D magnetic structure before and after major events, as determined from observation and modeling, (2) the physical cause of, and correlations among different types of solar activity (flares, filament eruptions, and Coronal Mass Ejections (CMEs)), (3) forecasting of solar activity – building on our long experience, (4) real-time prediction of the properties and dynamics of magnetic clouds resulting from CMEs, (5) study of coronal and interplanetary (IP) shock waves and their ability to accelerate energetic particles, in order to understand and forecast >10 MeV proton (solar energetic particle, or so-called "SEP") events, and (6) prediction of the likelihood and magnitude of geomagnetic storms and energetic particle events. Models of filament eruption will be tested in laboratory experiments in which filament eruptions will be simulated under controlled conditions. The laboratory experiment will be closely compared with results of observations and models, advancing our understanding of the underlying physics of CMEs, and providing new tools for predicting geomagnetic disturbances and SEP events.

Education of PhD students is an important part of this proposed work. We anticipate that at least 6 PhD students (including 3 proposed MURI fellows) will be trained by the 6 universities in the course of the project. These researchers will become members of the next generation of forecasters and scientists who build instruments.

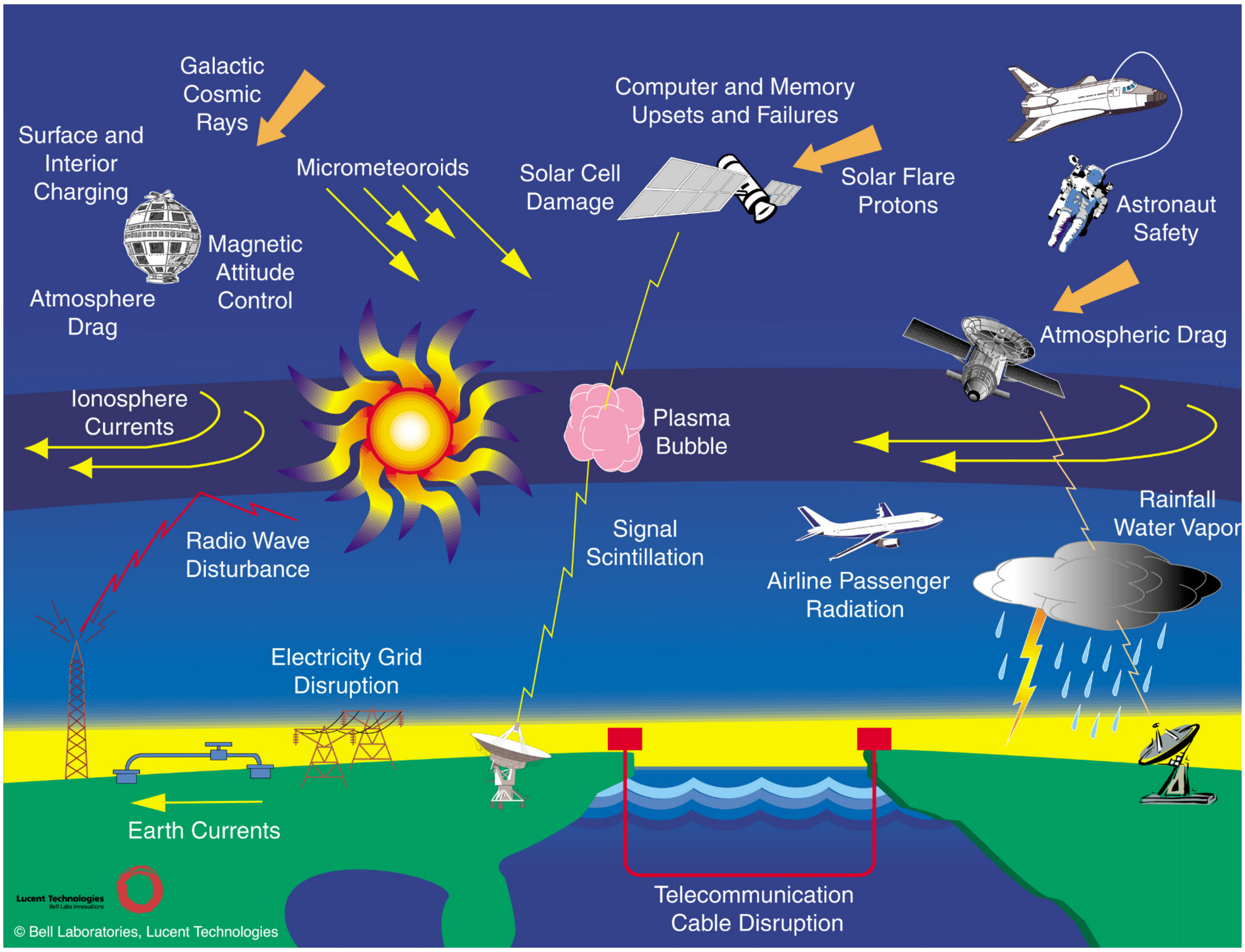


Fig. 1.— Overview of space weather effects on satellite and ground systems.

## 1. Overview

Figure 1 is the latest version of a widely known diagram by Lanzerotti (a member of this MURI team) that clearly illustrates the wide variety of space weather effects that can interfere with Department of Defense (DoD) and civilian assets. Almost all of these effects are directly due to the sun, or disturbances originating from the sun. Solar energetic particles (SEPs) affect spacecraft through solar cell damage, computer and memory upsets and failures, and surface and interior charging. Such particles also represent a significant radiation hazard to astronauts and airline crew on polar flights. Polar shortwave radio communication can be interrupted for days due to Polar Cap Absorption (PCA) from SEPs.

Solar X-rays cause sudden changes in the atmospheric drag on orbiting spacecraft, as well as ionospheric disturbances that affect shortwave communications and cause scintillation of satellite signals. The sun is the largest natural source of radio noise, and can affect cell-phone and wireless data transmission at the higher frequencies now being developed.

Magnetic bubbles (coronal mass ejections) drive compression of the magnetosphere, which in turn drives ionospheric and earth currents that can disrupt electric power grids and can affect other long conductors ranging from undersea cables to pipelines.

Strategies for reducing the impact of these effects rely chiefly on early warning, or prediction of impending events, so that satellites can avoid risky maneuvers, astronauts can seek safety, polar flights can be rerouted, and communications can shift to more "hardened" lines of communication. Equally important is the need for commanders to know that communication difficulties they may experience are the result of natural effects, and not the actions of an adversary. Another mitigation strategy is to use the knowledge gained in space weather studies to the design of satellite systems so that they will survive the largest event expected over their design lifetime.

In order to make reliable predictions or warnings with the maximum lead time, it is necessary to start at the source of the disturbances, the sun. It is also necessary to understand the physical processes that govern the long chain of events that lead from a disturbance at the sun to an associated magnetic storm or particle event at the earth. The above mentioned effects, even when due to a single event, may be spread over 2-3 days; the radiation effects occur immediately, the particle effects occur over hours to days, and the magnetic effects are delayed by 2-3 days from the start of the event. One or more of the ingredients, radiation, particles, or magnetic clouds, may be deceptively weak while another reaches dangerous proportions. Only through a deep physical understanding can one hope to recognize the signs of a developing threat in time for a meaningful prediction or warning, as well as place upper bounds on the magnitude of possible events which may occur over a period of years.

## 2. Introduction

The sun is the source of space weather – the disturbances whose radiative, field and particle energy directly impacts earth. Solar activity changes the radiative and particle output of the sun, producing corresponding changes in the near-earth space environment, as well as at the earth's surface. The most dramatic events on the sun, insofar as space weather effects are concerned, are solar flares and coronal mass ejections (CMEs).

A CME is due to a large scale rearrangement of the solar magnetic field which can induce a geoeffective solar wind structure. Each CME may carry away a mass of up to $10^{13}$ kg and release up to $10^{25}$ J of energy from coronal magnetic fields (Harrison, 1993 and 1995). Following their discovery, CMEs were soon found to be correlated with the occurrence of geomagnetic storms. CMEs are easily observed at the solar limb, where they are seen against a dark background. However, the earth-directed, disk CMEs are much harder to detect – although they are the ones that have the most important geomagnetic effects. Therefore, detecting the early manifestation of CMEs on the solar disk is essential to understanding earth-directed CMEs themselves. Establishing the correlation among the occurrence of CMEs and some other solar surface phenomena, such as filament eruptions and flares, is a long-standing problem in solar physics. After firm relationships are established (see §7.3), the correlated solar surface phenomena can provide an early warning of the occurrence of earth-directed CMEs.

In addition to the CME "magnetic bubble" itself, fast CMEs also drive interplanetary shocks that can generate a large number of high-energy particles. These shocks can extend up to 180 degrees in longitude, so that CMEs at all longitudes, including both the east and west limb events, can be associated with dangerous levels of particle events. Such SEP events are a significant space hazard, and understanding and predicting them is an important part of any space weather effort. Clearly, the common element of the magnetic and particle disturbances is the CME. Detecting and understanding the initiation of CMEs at the sun is the first element of our program.

CMEs have been studied using a number of coronagraphs since the 1970s, e.g. Skylab and Solar Maximum Mission (SMM). The launch of a new generation coronagraph – the Large Angle Spectroscopic Coronagraph (LASCO) on board SOHO – has provided the most advanced tool for studying the dynamics of coronal structure (Brueckner et al., 1995). With its improved sensitivity and a field of view covering a sun-centered region of 2 to 32 solar radii, LASCO has yielded observations of solar eruptions affecting the corona on a global scale. An ultimate goal is to establish the correlation between solar disk events (such as filament eruptions and flares) and geomagnetic disturbances. To do this, we will directly compare solar disk events with disturbances (in the form of magnetic clouds and particles) observed by ACE and Wind. During the course of our program, one can expect that next generation instrumentation will become available—NASA's Stereo mission, slated for launch in 2004. One of the goals of the first three years of our program will be to lay the groundwork for making optimal use of these new data.

The solar wind moves outward from the sun. The plasma and magnetic field of the solar wind interacts with the earth's atmosphere and geomagnetic field creating a teardrop shaped region called the magnetosphere. The surface of this region, referred to as the magnetopause, is at a distance of 5 to 10 earth radii in the sunward direction, and extends to distances beyond the orbit of the moon in the anti-sunward direction. The magnetopause represents a barrier that prevents all but a fraction of the energy carried by the solar wind from entering the magnetosphere.

Geomagnetic storms are a sustained ($\sim$several hours to days) response to a prolonged period of solar wind flow characterized by a strong, southward interplanetary field (see Figure 2). A storm is characterized by substantial intensification of the ring current that consists of trapped (10s to 100s of keV) ions and electrons at a distance of 2-5 earth radii. A ring current leads to significant geomagnetic depressions at low geographic latitudes. During storms there is enhanced precipitation of magnetospheric particles into the upper atmosphere, especially at auroral latitudes. Precipitating particles heat the neutral atmosphere generating traveling ionospheric

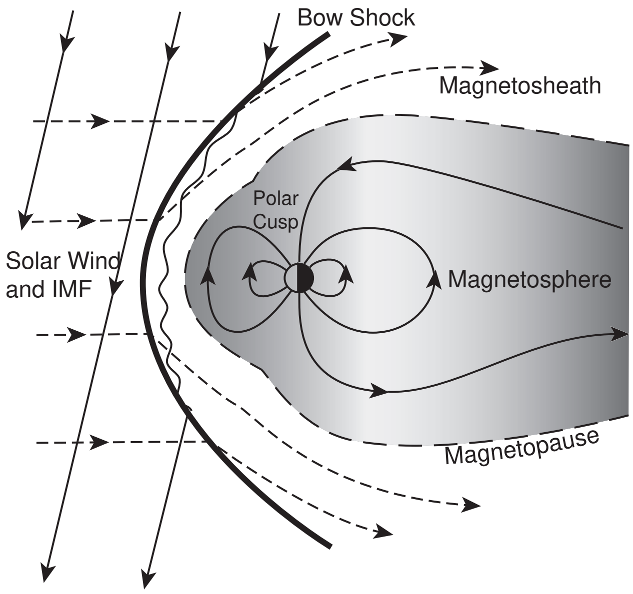


Fig. 2.— Schematic view of the interaction of the solar wind and interplanetary magnetic field (IMF) with the Earth's magnetosphere. The most geoeffective interactions involve an IMF with a substantial southward $B_z$ component.

disturbances (TID) that propagate from the auroral zone to mid-latitudes. Geomagnetic storms also frequently "pump-up" the energetic electron population in the radiation belts, both in number and energy. These electrons are the primary causative agent in total dose and bulk charging problems in the earth's magnetosphere. Geomagnetic substorms are characterized by a relatively short-lived ($\sim$20 minutes) impulsive response to solar wind stimulus. Substorms may occur during a geomagnetic storm, or in isolation, and are much more frequent than storms. Substorms frequently generate conditions in the geocynchronous (GEO) region conducive to charging spacecraft surfaces to high voltages.

Interplanetary charged particles ($\geq$10 MeV) that at times result from solar activity have deleterious effects upon assets and personnel that are flying in space. If these particles attain high enough energy (of order hundreds of MeV to over a GeV) they can also have implications for airliners on polar-latitude routes, including passengers and crew as well as the electronic systems.

SEP events in the GeV range have been of considerable scientific interest since their initial discovery by Forbush in the large solar event of 1942 (Forbush, 1946). It was the space age, however, that provided the opportunity to finally measure the characteristics of SEP events over their entire range of energies. While much space-based research on SEPs has been motivated by scientific imperatives, the fact that spacecraft systems, some with humans flying in them, are also exposed to such events means that there is considerable practical importance to better characterizing these events and understanding their origins. Indeed, a major U.S. conference in the 1960's that defined important directions for research in this field was motivated by the rapidly growing human space flight effort culminating in the Apollo program.

The surprising appearance of SEP particles with energy of a few MeV at GEO altitude (the expected geomagnetic cutoff is substantially higher), after solar events, was discovered (Lanzerotti 1968) soon after the launch of the first synchronous orbit test satellite, ATS-1. At that time, this finding had immediate implications for the design thickness of solar cell cover glass (Lanzerotti 1969) as well as for more general aspects of radiation hardening for communications or any other spacecraft that might subsequently occupy this orbital location. For example, today there are more than 200 active commercial communications spacecraft at GEO. There are also an unspecified number of DoD assets in this orbit, as well as in near-synchronous orbits and in highly inclined orbits that reach GEO altitudes. SEPs are also of immediate concern to spacecraft systems in low altitude, highly inclined orbits, including the International Space Station (ISS) and high-resolution, global surveillance spacecraft (e.g. Landsat).

Very prompt solar activity-associated charged particles can originate from a solar flare event itself. Such prompt events are often characterized by high relative abundances of $^3$He/$^4$He, highly ionized Fe and other species indicative of flare plasma (e.g. Reames 1999), and occur about 1000 times per year near solar maximum. Long-lasting (days) SEPs are now believed to derive a substantial portion of their extensive duration from the interplanetary acceleration of particles by shocks associated with coronal mass ejections (CMEs). Interplanetary shock-enhanced solar particles have been recognized since the first spacecraft measurements of SEPs, but their association with CME shocks has been of more recent vintage (e.g. Kahler et al. 1984). We note that a possible distinction between flare-produced blast wave shocks and piston driven CME shocks has been proposed (Wagner & MacQueen 1983; Cane & Reames 1988; Gopalswamy et al. 1998) and refuted (Cliver et al. 1998). Although CME-associated events measured at earth occur far less often (about 10 times per year near solar maximum) than flare-associated events, they reach higher energies and far higher fluences (integrated flux) than flare-associated events (e.g Reames 1999; Lee 2000), and so are more threatening to spacecraft and humans (e.g. Shea and Smart 1998).

Large enhancements in particle fluxes, of particle energy in the 100's of keV to several MeV, can often be measured as the driving shock wave passes the observing

Table 1
Primary Negative Impacts of Geomagnetic Activity on DoD Related Operations

| System | Activity | Impact |
|---|---|---|
| **Satellite Systems** | Energetic ions | Bit-errors in electronic signals/memory |
| | Energetic electrons | Internal and external charging, sparks, electrostatic or electromagnetic interference |
| **Power Systems** | Geomagnetic fluctuations | "Surges" in power lines |
| | | Massive power failures |
| **Navigation Systems** | Ionospheric disturbances | Location errors from maritime navigation systems such as LORAN and OMEGA |
| | Atmospheric scintillation | Position errors from the Global Positioning System (GPS) |
| **Communications** | Ionospheric disturbances | Outages of HF radio communication |
| | Solar Radio Noise | Increase in wireless (cell phone) dropped calls |
| **Air and Space Travel** | Energetic ions | Radiation hazard to aircraft and spacecraft crews and passengers |

location, and in fact, the energies of the shock-enhanced particles can reach many tens of MeV in some events. These shock-associated particles can comprise a substantial fraction of the total particle influence in a SEP, and can have serious environmental consequences for spacecraft systems, from solar cells to microprocessors.

Fortunately, these more dangerous events often develop relatively slowly, and their development may be predictable when sufficient information is available to determine a few key factors, such as (1) the speed of the associated CME relative to the local Alfvén speed, (2) the location and angular extent of the CME, and (3) relative geometry of the CME and interplanetary magnetic field.

Table 1 lists the primary negative impacts of geomagnetic activity on DoD related operations.

Predicting space weather, in particular geoeffective CMEs, is an important but difficult task. We believe that the next level of accuracy in prediction should incorporate physical parameters into the effort. This is the central task of the research proposed here. It is difficult to fully cover every aspect of the complex chain of interconnected events from initiation at the sun to final ground-level effects. We believe that a primary focus should be on the initiation and early detection of events at the sun, and on early identification of those events that develop into the earth-threatening variety in interplanetary space. We are fortunate that signs of this early development, if we can recognize them, will enable us to give warning well before the storm hits. Our team will focus on solar observations, and use heliospheric, magnetospheric, and ground-based measurements to provide a stringent, qualitative testing of our ability and progress in the prediction of space weather and its consequences to society.

Any operational (real-time) space weather prediction requires continuous monitoring of the solar surface with high resolution and high cadence. Especially, the vector magnetic structure of important active regions needs to be continuously monitored. In addition, correlative studies of CMEs with solar events has been hampered by incomplete coverage of the sun. We are working toward a unique capability to make 24-hour detailed observations through the use of three distinct, highly-automated observing networks – one making vector magnetograms, one measuring the sun in H$\alpha$ and the third measuring solar radio emissions. The networks are discussed in detail in §4.

## 3. Scientific Objectives

Our scientific objectives are to observe and forecast the initiation of space weather events, follow their propagation and development in the heliosphere, and predict their likely impact on the near-earth environment. We divide these objectives into two related parts: the study of geoeffective CMEs and the study of SEP events.

### 3.1. Geoeffective CMEs

Utilizing observations and modeling, we propose to address the following four objectives:

(1) Initiation of CMEs. We will combine observations and models to describe the solar magnetic and atmospheric configuration that leads to the onset of CMEs

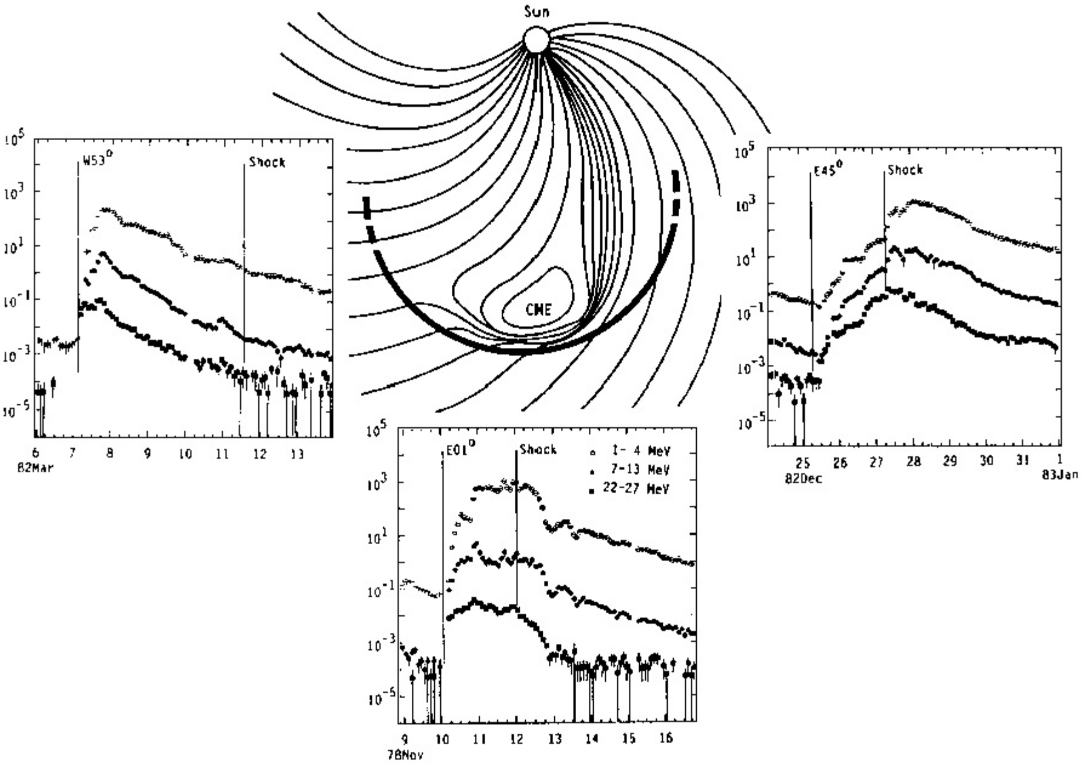


Fig. 3.— A figure from Reames et al. (1996), showing the spatial relationship between a typical CME and IP shock. The time profile of the SEP event observed in situ depends strongly on the solar longitude of the event, and on the evolving connection point between the shock and the spacecraft.

and associated surface phenomenon. Observations will be used as initial and boundary conditions for models. This is a critical ctep in predicting unstable conditions which would lead to the onset of CMEs.

(2) Propagation of CMEs in interplanetary space. We will follow the CMEs from the solar surface to 1 AU. Again, this will be done with both observations (solar and heliospheric) and models. The results will lead to the determination of important CME properties such as speed and magnetic field configuration during its entire propagation process.

(3) Geoeffectiveness of CMEs, and their relationship to solar surface magnetic configuration. Geoeffectiveness of CMEs will be evaluated by geomagnetic indices. If we follow the events from the sun to earth, we expect to track geoeffectiveness for all the events. This is very important for the space weather forecasts.

(4) Based on the results of (1) through (3), we will establish a system to predict the geoeffective CMEs. Here there are two distinct steps: (a) predict geoeffective events after the onset of solar events – this gives a 2 to 3 day lead time. (b) predict the onset of solar-surface events, by monitoring conditions that have the potential to produce geoeffective CMEs.

### 3.2. SEP Events

As stated earlier, there are two types of SEP events, (a) events due to solar flares, which are limited in spatial extent, have enhanced $^3$He/$^4$He ratios and (b) gradual events generated at IP shocks associated with CMEs, which are far larger in spatial extent, last longer, and occur far less frequently times per year during solar maximum (Reames 1999 and Lee 2000). Figure 3 shows how the time profile of SEP particles in gradual events depends on the longitude of the CME at the sun. Events at western longitudes (left box of Figure 3) rise rather abruptly to their maximum flux, then decline. Events at disk center (center box) rise almost as quickly, but reach a plateau (the "streaming limit" described by Ng and Reames 1994) well before the shock arrives. Events at east longitudes (right box) rise more slowly, and actually peak after the shock has passed.

Both flare-associated and gradual SEP events need to be included to predict SEP enhancements. Here our goals include understanding:

(1) Conditions for the generation of SEPs. We will combine observations and models of the magnetic and particle environment at the sun to understand condi-

tions that lead to the two types of SEP events. Conditions for generation of CME-associated SEPs are not well understood, but the essential parameters likely include the speed of the CME, the strength of the associated shock, and the geometry between the shock and the background IMF. Understanding the conditions for SEP generation will involve magnetograph, ground-based and space-borne coronagraph, radio, and solar wind observations, modeling of the solar and interplanetary magnetic fields, and theoretical investigation of acceleration of particles at turbulent shocks.

(2) Propagation of SEP particles. Once the SEPs are accelerated, their influence on the near-earth environment will depend on their propagation through the interplanetary magnetic field (IPM) and interaction with the magnetosphere. Relevant measurements will include multi-spacecraft observations of the particles at several locations in IP space, including elemental, isotopic, and charge-state observations, and also tracking of radio emission at the sun and in IP space. Propagation outside the region of the shock is relatively easily understood once the topology of the IPM is known, but confinement and propagation in the turbulent vicinity of the shock requires theoretical development. Understanding the propagation of particles is critical to any assessment of likely impact of the events on the near-earth environment.

(3) Geoeffectiveness of SEP events. After the arrival of the particles at the earth, their penetration into the magnetosphere and the polar regions of the earth's atmosphere is not well-understood. In situ observations of the particles (e.g. IMP8, GOES, and national security spacecraft), and observations of the magnetic fields at the earth's surface, as well as other magnetospheric storm indicators, will be used to shed light on these processes.

(4) Predictions of SEP events. Again we can consider two distinct steps, (a) forecasting the likelihood and severity of events at the earth once a solar event is in progress, and (b) predicting the likelihood of a SEP event based on developing conditions at the sun and in IP space. Such predictions must be based on a better understanding of the physics involved, and on an array of real-time observational tools. We are confident that such an approach will lead to improved methods of forecasting, and also to a better understanding of which observations are most essential in forecasting.

## 4. Observing Tools

### 4.1. Vector Magnetograph Network

Any viable space weather program must be a full-time operation. We already have experience in establishing and operating a round-the-earth network (see §4.2). It is important that we be able to observe magnetic fields around the clock. SOHO MDI provides continuous magnetogram data, but it measures only line-of-sight fields, and the cadence is typically 90 minutes. The USAF Improved Solar Observing Optical Network (ISOON) is nearing installation, and two sites (Holloman AFB, NM and Learmonth, Australia) should be operational by the end of 2001. ISOON will supply fully processed 2K×2K full-disk images in near real-time, on-line, in H-alpha, continuum, and line-of-site magnetic fields. The ISOON system is described in Neidig et al. (1998). Neidig is PI on the ISOON project and is a co-investigator on this MURI proposal. High-cadence 24-hour network observations of *vector* fields would provide a unique tool. Here we propose a three-station vector magnetograph network composed of stations at BBSO, Huairou Solar Observing Station (HSO) of Beijing Observatory in China and the Instituto de Astrofísica de Canarias (IAC) in Tenerife, Spain. The three are about eight hours apart and have staffs that are very experienced in vector magnetography.

BBSO and HSO have long experience in coordinated round-the-clock magnetograph observations. Under our NSF-INT supported US-China collaborative research program, we have had very productive years on several projects, centered on studies of vector magnetic fields. These are high-resolution observations with a field of view sufficient for studies of individual active regions. Full-disk vector field measurements are currently unavailable, but are expected to be available openly and in real-time (but at lower resolution and from only one station) within the next two years from the SOLIS (synoptic optical long-term investigations of the sun) instrument. We will incorporate SOLIS data when available, but the high-resolution network described here will remain essential for detailed studies. Combining BBSO and HSO observations, we have limited our night gap to 4 hours in the summer, and 8 hours in the winter. The partnership of the IAC will enable us to achieve true "round-the-clock" observations. IAC, in the Canary Islands, is an ideal partner for us because: (1) their site has an established reputation of excellent observing conditions and productive research; (2) they will provide a telescope and a narrow bandpass filter for the magnetograph; (3) they will operate the telescope at no cost; (4) they will actively participate in space weather research. With this station, we will have three stations placed uniformly around the world to give high cadence vector magnetograms around-the-clock and year-around (for IAC this network will be year-around like the helioseismology networks they operate). In this proposal, we include a small amount of money in the budget for a computer, a liquid crystal modulator and a 12-bit Silicon Mountain Design (SMD) camera to complete the system. The system would be a duplicate of the BBSO system, so the effort for its development is minimal.

Our operating two-station network is composed of the BBSO Digital Vector Magnetograph (DVMG) system, and the videomagnetograph (VMG) at HSO. Recently, we completed the critical steps for the new BBSO DVMG – replacing the optical train with one having no moving parts, and replacing the video camera with a 1K×1K 12-bit SMD digital camera. We anticipate that this Lyot filter based DVMG will be complemented by a second, Fabry-Pérot based imaging vector digital magnetograph (IVDMG) by Spring 2002. The DVMG will reside on our 25 cm telescope and the IVDMG on our 65 cm telescope. The latter will be used for highest resolution work. The 25 cm telescope has about a 300×300″ field-of-view (FOV). This is comparable to the FOVs of our partners. Our 65 cm high-resolution telescope has a FOV of about 150×150″ Since we do not have full-disk coverage, we will concentrate on studies of the most promising regions. However, each site will do three disk scans per day to cover all active regions, so that we have nine scans per 24 hours. Figure 4 shows a sample digital vector magnetogram from the DVMG system. The background is an H$\alpha$ image during an M2.3 flare of October 26, 1999. The cross-talk and instrument polarization have been minimized in the data with our new system.

The BBSO DVMG system uses a narrow photospheric spectral line, Ca I 6103 Å line ($g_L = 2.0$). The center of the bandpass is set at $\Delta\lambda = 110$ mÅ on the blue side of the spectral line. The temporal and spatial resolution of BBSO vector magnetograms depends on the number of individual frames that are combined to produce them. The old BBSO VMG system, which was quite like the HSO system, had a time resolution of about 1 minute, and a spatial resolution of 1-2″. The calibration of the system was described by Varsik (1995).

Last year, we received a DURIP award to develop a filter based IR magnetograph by combining a Fabry-Pérot and Lyot filter – the imaging digital IR vector magnetograph (IRDVMG). For us, DURIP support opens a new and powerful avenue of studying space weather. This IR system will be the first in the world using a narrow band (2.8 Å) Lyot prefilter. In this context, narrow means narrower than the free spectral range of the Fabry-Pérot. This system will have the same optical set-up as the visible light system. Before this IR system, the lack of a narrowband IR prefilter forced others to more complicated and difficult systems (like ones with multiple Fabry-Pérots). IR polarimetry, once our rugged technology is in place, will have several advantages over visible light field measurements. First, we see deeper into the sun because of the opacity minimum near 1.6 $\mu$. Second, the Zeeman splitting increases as the square of the wavelength, enabling a more precise measurement of the field than with visible light. Third, the effect of terrestrial atmospheric turbulence, or "seeing", decreases with increasing wavelength ($\propto \lambda^{\frac{6}{5}}$), so that we have better images. In sum, we will measure magnetic fields more accurately, which is critical to testing models in §5 – requiring magnetic field measurements as boundary conditions.

**M 2.3 Flare on October 26, 1999**

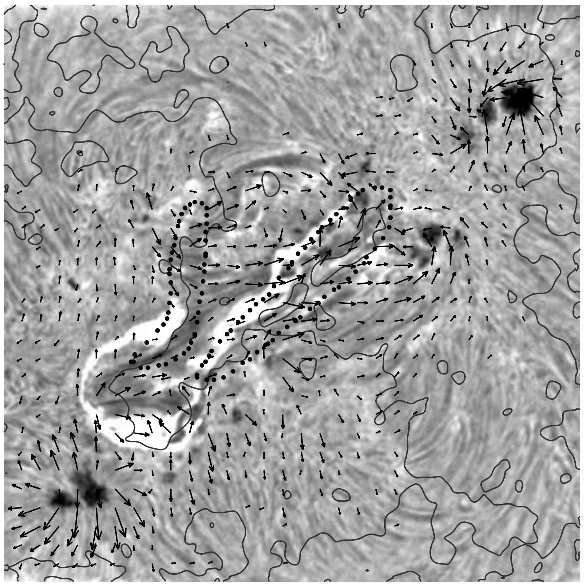

**FOV 174"x174"**

Fig. 4.— A vector magnetogram from October 26, 1999. The background is an H$\alpha$ image during the M2.3 flare. Arrows mark the transverse fields, and the solid lines are neutral lines of line-of-sight magnetic fields. Strong magnetic shear is clearly visible in the areas near flare ribbons, as circled by dotted lines.

The VMG system at HSO was developed by Ai (1987). It is very similar to the old BBSO VMG system, except that it uses the Fe I 5324 Å line ($g_L = 1.5$), and sets the filter at $\Delta\lambda = 75$ mÅ from line center. The bandpass of the birefringent filter is 1/8 Å. Like the BBSO magnetograms, the temporal and spatial resolution of its magnetograms depend on the number of frames added. The combined HSO and BBSO system has been used many times for coordinated, round-the-clock observations (Wang et al., 1989).

The Observatorio del Teide, which is located at an elevation of 2400 m on the island of Tenerife, is the observatory with the best conditions for solar observations in Europe. Due to its high elevation, it is above the inversion layer, thus enabling high quality observations under excellent seeing conditions. IAC operates the solar laboratory, which has the form of a pyramid aligned in north-south direction. It houses a suite of different instruments for the continuous observation of solar oscillations (e.g., GONG, TON, BISON, IRIS, ECHO). This pyramid is the ideal place to install and operate another high-resolution CCD camera of the global H-alpha network, currently consisting of three different sites (see next section), as well as one system of the planned magnetograph network for year-round observations. The sunlight is fed by a small coelostat into the interior of the solar laboratory, where the optical systems for the H$\alpha$ and magnetograph cameras will be installed on two optical benches. The computers controlling the cameras will conveniently be located in the observing room. The experience of the observing staff and the stable weather conditions will guarantee the successful operation of both instruments.

### 4.2. Global High Resolution H$\alpha$ Network

Based on our successful experience in making high resolution full-disk H$\alpha$ observations at BBSO, and the urgent need to monitor the solar activity continuously, we have deployed a network for H$\alpha$ full-disk observations utilizing existing facilities at BBSO in California, Kanzelhöhe Solar Observatory (KSO) in Austria, and Yunnan Observatory (YO) in China. This effort has been partially supported by NSF's space weather program. All three observatories have over 300 sunny days a year, good seeing conditions, experienced observing staffs and well-established H$\alpha$ telescope systems. We have replaced the film systems in KSO and YO with 2K$\times$2K digital cameras. At BBSO we installed a new 2K$\times$2K digital camera with 14 bits instead of 8. We have provided KSO and YO with the data reduction software and analysis techniques already developed at BBSO, which significantly improved the data quality, while providing a consistent and linked data set. KSO and YO are providing the manpower required to collect and reduce their data. With this network, we can monitor solar chromospheric activity with $1''$ pixel resolution and one minute cadence, round-the-clock, for most of the year, with the data quality shown in Figure 5. Three systems were built at BBSO, and have been deployed. The three observatories are in ready e-mail contact for prompt forecasting and reporting. Detailed exchange of full data sets are done on a weekly basis. Figure 6 shows the comparison of observations from the three stations on the same day.

Two more stations are currently being added to the network. An identical system to the Yunnan system is established in Huairou observing station of Beijing Observatory. The longitude of Beijing is not much different from that of Yunnan, however, the climates are very different. So the combination of these two stations provides an excellent duty cycle for the China time zone. The instrument and operation funding for the Huairou site is provided by the Chinese National Science Foundation. IAC in the Canary Islands is building the fifth system. The IAC will provide the telescope, filter and observers, while we will apply in the instrument option for the 2K$\times$2K camera. We will also provide our image processing software (see Figure 5 for a typical processed BBSO image). The IAC $H\alpha$ data will be an excellent complement to that from KSO. Please note that even if option funding is not approved, the four-station network will still achieve most of our objectives. Furthermore, many of our proposed studies using our network will be strongly complemented by the H$\alpha$ component of the ISOON network when it is on-line.

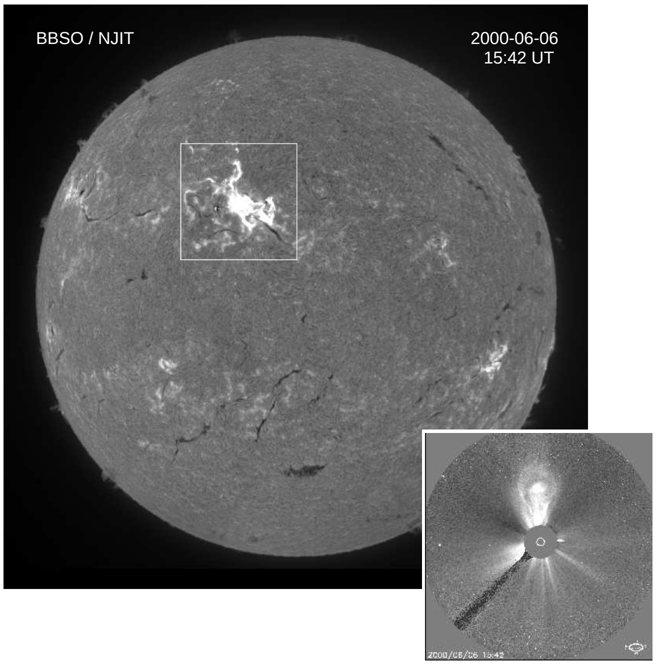


Fig. 5.— Contrast-enhanced full-disk H$\alpha$ image (2K$\times$2K pixel) obtained after correcting for dark current and after subtracting the average center-to-limb variation of the quiet sun. This image was recorded at BBSO on June 6, 2000, at 15:42 UT during the eruption of an X2.3 flare in NOAA 9026. This flare, whose position is marked by the white box (400 $\times$ 400 pixel), started at 14:46 UT and was associated with a halo CME and a severe magnetic storm. The inset in the lower right corner shows this magnificent CME on a SOHO/LASCO C3 image recorded at the same time, although the contrast of the halo is quite weak.

### 4.3. Microwave Radio Network

A substantial fraction of CMEs are time-associated with solar flares, which produce copious high-energy particles. In addition, solar flares that are at western solar

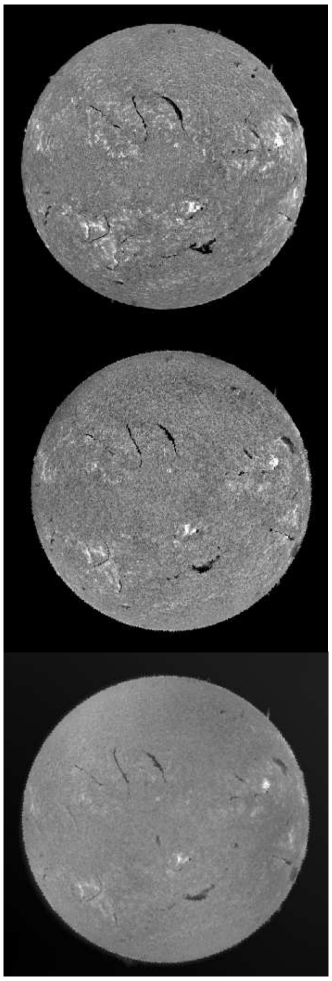

Fig. 6.— This series of contrast-enhanced H$\alpha$ images was obtained on August 23, 2000, at Yunnan Astronomical Observatory (03:11UT, bottom), Kanzelhohe Solar Observatory (06:37UT, center), and Big Bear Solar Observatory (15:46UT, top). Note the evolution of the filament in the southern hemisphere within only a few hours.

longitudes, and so magnetically well-connected to earth, can be the direct source of prompt SEP events. Solar radio noise is also implicated in some wireless (cell phone) network outages. A sensitive way to detect the occurrence of such events, but not their location on the solar disk, is through the radio emission they produce, which can be detected easily with inexpensive ground-based radiometers, *even through clouds*, and even from events some distance beyond the solar limb. Any real-time, round-the-clock monitoring system should include a radio component, to ensure detection of radio bursts associated with solar flares, and even sometimes with erupting filaments without a substantial optical flare. Such events, however, may vary greatly in the radio frequency of their strongest emission, and monitoring activity at several widely-spaced radio frequencies can still miss or cause underestimation of the strength of events. A broad-band, multi-frequency capability with round-the-clock coverage is needed.

At NJIT, we run the Owens Valley Solar Array (OVSA) in California, an imaging instrument that operates between 1 and 18 GHz. This instrument was the motivation behind the development of the Solar Radio Burst Locator (SRBL) prototype that is supposed to be developed into a multi-station network by the US Air Force, and the one presently operating station is located also at the OVSA site. The mission of the SRBL network is to provide approximate (within 2 arcmin) locations of rather intense bursts, $>$ 500 solar flux units (SFU), which limits its operation to one polarization, with less than optimum sensitivity. We have completed the design and are constructing a Solar Radio SpectroPolarimeter (SRSP) based on the SRBL design, but with dual polarization capability and increased sensitivity. These improvements make the SRSP better for detecting the weaker events, and ensure that no highly polarized events are missed due to observing in the "wrong" polarization. This first SRSP, constructed at NJIT, will be operated at Bell Labs (Murray Hill, NJ) by team member Lanzerotti beginning early 2001. We believe a three-station network of SRSPs would be an ideal complement to a future SRBL network, can be implemented sooner than SRBL, and will provide essential information for this MURI project, giving the radio flux and polarization spectrum of *every* solar burst down to about 10 SFU. Such spectra will be used to characterize the acceleration of high-energy particles at the sun, through established gyrosynchrotron emission diagnostics, and to provide statistical measures for association with other properties of CMEs and SEPs. Although Kundu & Haddock (1960) and Castelli et al. (1967) proposed that certain radio spectral characteristics might be associated with polar cap absorption (PCA) events, a study with a larger number of events (Cliver et al. 1985) showed little direct correlation of SEP occurrence with microwave spectral shape. However, the more detailed and sensitive microwave data that would be provided by OVSA and by a network of SRSPs (see Figure 7) could provide new, if more subtle, links between the two.

For example, the accelerated particles that give rise to the microwave radio bursts may be important as seed particles in shock acceleration. At the lowest frequencies near 1 GHz, we will see radio emission from higher in the corona, to mark the presence of some activity that may be indicative of an eruptive event. Therefore, data from the radio network will be useful for verifying whether energetic particles are present from an associated flare or not. Although some SEP events are due to shocks with no apparent associated flare, it may be that seed parti-

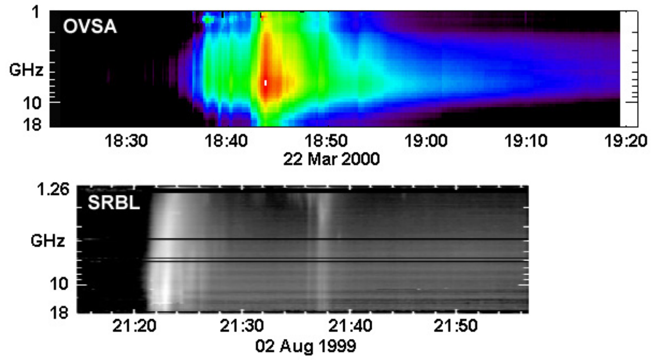


Fig. 7.— Microwave spectra from OVSA (upper panel) and SRBL (lower panel) for two different radio bursts from CME associated flare. The SRSP network will be more sensitive than SRBL, and will provide data in both senses of circular polarization, but has the same 1-18 GHz coverage as both OVSA and SRBL.

cles come not from an associated flare itself, but from a previous flare event. Continuous coverage of flare events will be essential to determine such delayed associations.

### 4.4. Other Ground-based Radio Facilities

A variety of distinctive radio signatures are often generated in association with major solar eruptive events. These radio signatures can provide remote sensing tools for specifying and forecasting the space environment associated with such events. The ground-based and space-based radio signatures, taken together, give a global view of the entire space weather system.

To clarify and identify the sources of energetic particles high in the corona, we need to combine data from decimetric, metric and space-based (decametric and longer wavelengths) radio observations. At metric wavelengths, which penetrate the earth's ionosphere and so are observable from the ground, we can directly detect the presence of a shock from type II signatures. (A type II burst is one whose emission drifts to lower frequencies with time, due to the exciter shock wave traveling outward through the corona.) Many of these type II signatures also have associated herringbone structures, which are direct evidence for particle acceleration. Additional evidence of shock acceleration is given by type IV radio bursts. The metric observations thus provide measurements of near-sun, high-energy particles at the right height and location to supply seed particles to the shock. Other types of metric radio emission such as type III (electron beam) emission are not directly related to the particle-accelerating shock, but provide information on timing of energy release and relative numbers of energetic particles at the sun. Such observations will be obtained from the Nancay Radioheliograph (team member Pick), and from existing spectrometers located around the world, some of whose data are available in near real-time.

Unfortunately, there is a gap in ground-based coverage of metric radio emission at US longitudes, since no solar meter-wave spectrometer currently exists at these longitudes. In contrast, the low-frequency ($< 14$ MHz) space-based observations of the sun have continuous time coverage. This means that for some of the space-based observed solar radio emissions there is no corresponding ground-based (metric) coverage. To remedy this, we propose here to build and install a low-cost spectrograph system in the US based on the successful and highly-automated system at Culgoora, Australia. The US Air Force is currently deploying a Solar Radio Spectrograph (SRS) system as part of the ISOON network, and the SRS is also based on the Culgoora system. But the SRS employs low-gain antennas, whereas the system we propose would use high-gain, sensitive antennas. The system, using largely commercial components, will be assembled under the direction of our team member White at UMd, and is expected to be deployed at the radio-quiet Green Bank, WV site, with the help of Dr. Timothy Bastian, of the National Radio Astronomy Observatory (NRAO). Together with the Culgoora spectrograph in Australia, and the Nancay spectrograph, we will have round-the-clock, high-sensitivity coverage of metric type II, III, and IV bursts. This, in combination with the SRSP network discussed above, will give us complete ground-based radio coverage from the low-frequency ionospheric cutoff up to 18 GHz.

### 4.5. Low Coronal/Interplanetary Magnetic Field Topology

Once a CME is launched from the sun, it and its associated shock interact with the large-scale magnetic field in the corona from, say, 2-30 $R_\odot$, and later with the large-scale IMF. Strong SEP events begin producing particles in the low corona. The presence of a strong radio burst indicates flare acceleration that may be critical in providing the seed particles that in turn generate the turbulence that allows diffusive acceleration at the shock. We think it likely that a truly SEP-effective shock depends not only on speed and shock strength, but also on this initial geometry in the low corona. We will use active-region-scale magnetograph data from the magnetograph network discussed above, but also large-scale magnetograph data from MDI onboard SOHO and upgraded GONG (and ultimately from SOLIS) as input to model the magnetic environment in the low corona through which the shock must pass.

### 4.6. Coronal Observations

Many of the key observations can be performed only from space, including coronagraph observations at $> 2R_\odot$, decametric and kilometric radio observations, and in situ particle measurements. Our MURI team includes experts in each of these areas who are closely associated with key spacecraft. Some of the space data discussed below will be publicly available, and will not be unique to our team. However, a number of our team members have close association with various experiments and can provide unique experience in utilizing these data sets.

To monitor coronal surface structures associated with CMEs, we will rely on data from EIT/SOHO which provides transition region and lower coronal loop structure, and mass loss (dimming after major events), and from Yohkoh SXT which provides important information about the structure of hotter plasma than observed by SOHO/EIT. The SXT data will be used to guide force-free extrapolation of 3-D magnetic fields. It is also possible to construct magneto-hydrodynamic field topology using numerical relaxation methods (Wu et al., 2000). In addition, TRACE data provide higher resolution observations for the transition region and the lower-temperature part of the corona.

To monitor the structure of CMEs themselves, we will initially use LASCO/SOHO data. In early 2004, two Stereo spacecrafts will be launched. More comprehensive data for CMEs will be provided by the twin satellites from different views. Dr. Plunkett (member of this MURI team) is a key member in both LASCO and Stereo instrument teams.

### 4.7. Interplanetary Magnetic Clouds Observations

Interplanetary magnetic cloud data are routinely obtained by Wind and ACE. The key data sets are from magnetometers from these two missions. The magnetic structure of magnetic clouds can be derived based on the temporal evolution of vector magnetic fields. Dr. Chen of NRL, and member of this MURI team is an expert in interpretating these data sets.

### 4.8. Index Data For Monitoring Geoeffectiveness

In recent years, several arrays of magnetometers have been established at high geomagnetic latitudes in both polar regions. The purposes of these arrays are severalfold, including as a prime objective the understanding of the interaction of the solar wind with the magnetopause. By virtue of their high geomagnetic latitude locations, at the base of magnetic flux tubes that thread the magnetopause, the variations in the geomagnetic field can be studied in the context of the solar wind in its encounter with the magnetosphere.

One of the members of this team of MURI investigators (LJL) is a PI for eight magnetometer instruments that are located in the Antarctic at South Pole (SP) and McMurdo (MM) stations, and in the six United States Automatic Geophysical Observatories (AGOs). These locations range from auroral (about 65° geomagnetic) to the polar cap (two AGOs located at about 86° on both sides of the corrected geomagnetic dipole pole). Each AGO site (as well as the manned stations at SP and McMurdo) is instrumented with a suite of geophysical instrumentation that includes imaging riometers, search coil and fluxgate magnetometers, all sky cameras, and ELF and VLF receivers. Data from these instruments provide a comprehensive description of high latitude geophysical variations on geomagnetic field lines at, and on the magnetopause.

Numerous models and empirical studies have concentrated on the conditions that can result in large geomagnetic storms as recorded by large changes in the magnetosphere ring current as expressed by the geomagnetic Dst index (degree of equatorial magnetic field deviation, by ground stations). These are very valuable studies in that a large number of impacts on technical systems can occur during large Dst events. Indeed, it can be confidently asserted that no significant impacts of the solar-terrestrial environment on technical systems have been found to occur under quiet Dst conditions. Other indices from NOAA such as Ap and Kp indices will also be evaluated.

### 4.9. Space Particle and Plasma Observations

Measurements of interplanetary particles are now being made on a number of spacecraft, and the data become available for analysis after various delays following their acquisition. Charged particle data of particular relevance to this MURI program are available from instrumentation on the SOHO, WIND, ACE, IMP8, and Ulysses spacecrafts. The first three of these are located upstream of earth orbiting about the L1 Lagrangian point. The IMP8 spacecraft is in orbit around earth and Ulysses is in a solar polar orbit, making its second south solar pole pass in September 2000.

Interplanetary electron and proton data (as well as magnetic field data) from ACE are routinely used by the NOAA Space Environment Center (SEC) as part of their prediction and warning program. These particle data are derived from an instrument that is the backup to a solar particle instrument on the Ulysses spacecraft for which a MURI co-investigator is the PI (LJL). Another of our MURI co-investigators (Blake) is a co-investigator on another Ulysses particle instrument. The Ulysses spacecraft in its polar orbit is not directly in the "line of attack" of a solar-originating charged particle event that is about to strike earth. Yet, data from Ulysses has proven extremely important in defining some of the physics of high helio-latitude solar events and CMEs that themselves can produce energetic particles that can also reach earth.

In terms of a global, heliosphere-wide understanding of interplanetary charged particles, this MURI team is also collaborating in particle investigations on the outer planet Voyager 1,2 spacecraft (now both beyond 50 AU distance) and on the Cassini mission to Saturn (presently located at 5 AU enroute to its Saturn encounter in 2004). This MURI team thus has ready and direct access to data from six interplanetary spacecraft by virtue of its direct involvement in the programs of ACE, IMP8, Ulysses, Cassini and Voyager 1,2 (in increasing distance from the sun). This means that this MURI team will remain on the forefront of solar and interplanetary particle physics investigations for the duration of this MURI program (Lanzerotti et al. 2000).

In addition to data on the fluxes of electrons and protons, the ACE, Ulysses, Cassini, and Voyager instruments also provide fluxes of the composition of the interplanetary ions for species from He to Fe. These data can be used with solar wind composition data to derive understanding of interplanetary shock effects on particle acceleration (e.g., Gloeckler et al., 1994).

Team member Zurbuchen manages a multi-spacecraft data-center for solar wind and energetic particle monitors. He has access to near-real-time data on solar wind plasma composition from ACE, Wind and Ulysses that can be related back to the solar surface. Such data provide, in effect, a continuous monitor of one measure of the interplanetary magnetic field topology, as well as give coronal density and temperature diagnostics based on the elemental and charge state determinations (Zurbuchen et al., 1998, 2000).

The elemental and charge-state composition of the solar wind will be used to distinguish the magnetic topology of the solar wind source region at the sun. When loops emerge from the photosphere, they appear to have essentially photospheric composition. Elements of low first ionization potential (FIP), such as Mg, are found to be enriched in the corona (Feldman et al., 1998; White et al., 2000) on a time-scale of $10^6$s. A possible FIP fractionation process that occurs in closed magnetic structures has been discussed by Zurbuchen et al. (1998). A similar elemental fractionation is found in low-speed solar wind, but with a large degree of variability due to its source, which is a conglomerate of individual plasma streams originating from discrete coronal magnetic structures that are opened (presumably) by magnetic reconnection. Solar wind that originates in coronal holes, in contrast, can be readily distinguished by its more steady composition, and the absence of enrichment of low FIP elements. These characteristics allow mapping of the interplanetary magnetic topology back to the solar wind source region, as distinguished from other changes in the solar wind that might be caused by, for example, stream-stream interactions.

Ionic composition of the solar wind depends on the temperature and density profile in the low corona. For CMEs, the temperature history and plasma processes near the source in the low corona often differ markedly from those measured in fast and slow solar wind streams. Shown in Figure 8 is the ratio of $O^{7+}$ to $O^{6+}$ vs. the average charge-state of solar wind iron, as seen from ACE/SWICS between day 296 and day 305 of 1998. The different solar wind types and the hot ejecta of CME material are readily separable. In addition, it has been shown that $\sim$ 50 % of CMEs at earth are associated with unusually high charge states in Fe. Such unusual charge-states result from plasma heating close to the sun. Direct comparisons with solar data, as described above, will provide additional constraints on heating and expansion effects of CMEs, measurements directly relevant for the prediction of their impact on earth. Equivalently, the occurrence of an unusually cold charge state composition of the solar wind (see, e.g., Gloeckler et al., 1999) marks plasma that originates from initially cold coronal structures, such as from erupting filaments. In this case, the relationship between the leading edge of the interplanetary CME and the associated erupting filament can be directly studied.

Solar wind plasma and compositional data will be used to characterize the propagation of CMEs through the interplanetary medium. Once the different components of the three-part CME structure are compositionally identified, we can compare the in situ measurements of magnetic field direction and other plasma parameters in each part (i.e. near the shock, within the CME front, and within the filament material itself). Comparisons can then be made with measures of geoeffectiveness to determine what part of the CME structure plays the largest role in the magnetospheric perturbation.

### 4.10. Space-based Radio Emission

The space-based Wind (Bougeret et al., 1995) and Ulysses (Stone et al., 1992) platforms have state-of-the-art matched synthesized radio receivers that provide remote observations of radio sources propagating through the interplanetary medium. Wind has radio receivers that cover the frequency range from 4 kHz to 13.8 MHz, which corresponds to radio emissions generated from near the sun to beyond 1 AU. The Wind spacecraft is

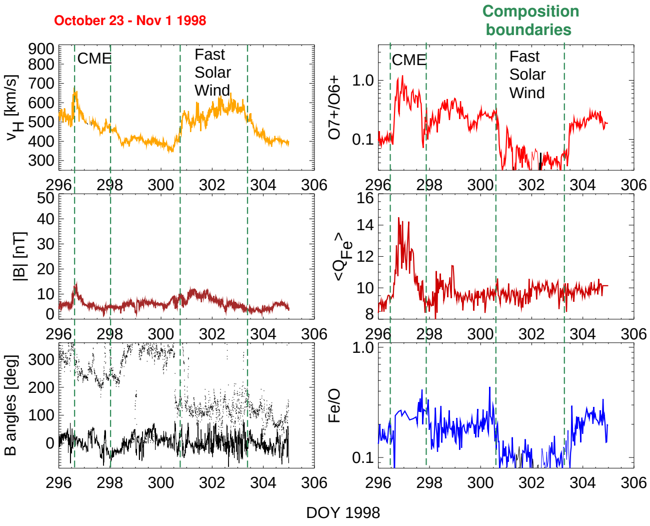


Fig. 8.— ACE/SWICS data for October 1998, showing the differences in signature of CME plasma, slow, and fast solar wind. Both the CME and fast solar wind have relatively high solar wind speed ($v_{\rm H}$, upper left panel), but markedly different temperature (as deduced from, e.g. $O^{7+}/O^{6+}$, upper right).

on a variable trajectory that takes it from near-earth orbits out to about 200 $R_E$ from earth. Ulysses' radio receivers range from 1.25 kHz to 940 kHz. Ulysses is in an elliptical solar orbit, out of the ecliptic plane, with aphelion (perihelion) at $\sim$ 5.4 AU ($\sim$ 1.3 AU). Both spacecraft have direction finding capabilities that can assist in locating the source of the radio signals in the interplanetary medium, and therefore, can help to distinguish those disturbances that are headed toward earth. The radio receivers on both spacecraft can also detect the in situ phenomena (such as shocks and Langmuir waves) that are associated with the generation of radio emissions from the remote radio sources. The twin spacecraft of the upcoming STEREO mission will each have a radio receiving system based on the Ulysses/Wind/Cassini heritage.

#### *4.10.1. Radio signatures associated with the coronal and interplanetary propagation of CMEs*

Metric type II radio bursts, which correspond to the propagation of coronal shocks, have been observed from ground-based radio observatories since the early 1950s (Wild, 1950). Their relationship to CMEs is not yet firmly established, as mentioned earlier. By contrast, the interplanetary (or kilometric) type II radio bursts (Malitson et al. 1973) observed from space-based platforms in the frequency range from ~20 kHz to ~1000 kHz, are known to be generated by electrons accelerated at CME-driven shocks propagating through the interplanetary medium (Cane, Sheeley and Howard, 1987). More recently, the gap between the high-frequency ground-based and low-frequency space-based radio observations has been nearly closed by the high-frequency receivers on the Wind/WAVES experiment. The decametric to hectometric type II radio bursts observed by Wind/WAVES are providing new insights into the formation and dynamics of the CME-driven shocks in the high corona.

The type II radio signatures of CME events provide crucial and unique information on CME propagation and speed during the entire period of interplanetary transport from the sun to earth. Their observed frequency drift rate is directly related to the speed of propagation of the coronal or interplanetary shock. The study of the type II signatures in the frequency range from 1 to 14 MHz is important because these radio observations correspond to coronal heights that overlap with the white-light observations from LASCO (Reiner et al., 2000*a*). Unlike the LASCO CME measurements, which give the CME speed projected onto the plane of the sky, the frequency drift rate of the type II radio emissions corresponds to the "true" speed of the CME, provided that the coronal density profile is known. (In principle, the background coronal density profile at any given time can actually be measured from the LASCO coronagraph images). The inter-calibration of the LASCO and radio observations can thus provide crucial information on the true speed of the CME/shock as it moves from the solar corona into the interplanetary medium.

The interplanetary (kilometric) type II radio emissions provide the only current means of remotely tracking CMEs through the interplanetary medium from $> 30 R_\odot$ to earth – beyond the range of white-light coronagraph images. These remote radio observations can therefore provide a more accurate prediction of the arrival time of a CME at earth. Reiner et al. 1998 have developed techniques to facilitate the tracking of the CMEs using the interplanetary type II radio emissions. Reiner is a co-investigator on this MURI team. The direction-finding capabilities on Wind and Ulysses have also been used to locate and track the type II radio source regions for earth-directed CMEs. The low-frequency radio tracking and triangulation of the radio signatures of CMEs will be continued on the NASA STEREO mission, which is specifically designed to study and track earth-directed CMEs from stereoscopically-spaced spacecraft located at vantage points both leading and lagging earth in its orbit about the sun.

Figure 9 reveals the correspondence between a CME observed by the SOHO/LASCO coronagraph and the associated type II radio emissions. The CME was observed from $\sim 3R_\odot$ out to 18 $R_\odot$, i.e., from the high solar corona to the interplanetary medium. Over this range of distances, the propagating CME generated radio emissions from the decametric to near-kilometric wavelength regimes. Once a method for converting the observed radio frequency to a scale height is established, the dynamics of the CME, as described by the linear relationship between the height and time (shown in the insert), can be directly compared to the dynamics implied by the frequency drift rate of the type II radio emissions. The white curve on the radio dynamic spectrum, which passes directly through the decametric and hectometric type II radio emissions, corresponds exactly to the height-time relationship measured for the observed LASCO CME. This one- to-one relationship between the type II radio emissions and the CME clearly demonstrates that the radio emissions can be used to track CMEs from the solar corona to the interplanetary medium. Thus, the radio observations complement and extend the range of the white-light coronagraph images.

### *4.10.2. Radio signatures and the initiation of CMEs*

A major solar flare that also involves the liftoff of a CME is usually accompanied by a complex, fast-frequency-drifting kilometric type III radio burst (sometimes also called a Shock Associated (SA) event (Cane et al. 1981, Bougeret et al. 1998). These complex type III bursts are usually the first radio signatures indicating the liftoff of a CME on the sun. Reiner and Kaiser (1999) have found that the observational characteristics of these complex type III bursts, in the frequency range between 1 and 14 MHz, are distinctly different from ordinary type III radio bursts that are only associated with a solar flare. Furthermore, by comparing hectometric type III profiles with the decimeter wavelength radio emissions in the 1-3 GHz region, Reiner et al. (2000*b*), demonstrated that at least some of these complex type III bursts were produced by energetic electrons accelerated at the flare site, as also noted by Kundu and Stone (1984), and not by electrons accelerated at blast-wave shocks as has been previously proposed.

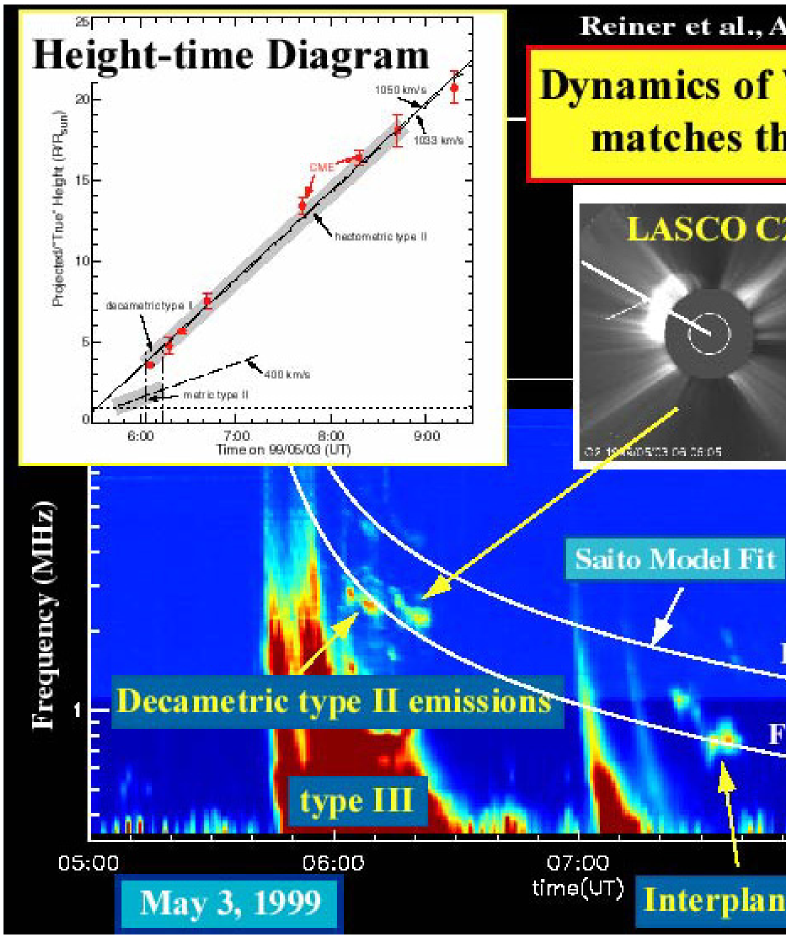


Fig. 9.— Overview of a CME and associated decametric radio emission from the Wind spacecraft, for an event on 1999 May 03. The relationship between frequency of emission and local electron density is used to track the shock wave as it moves outward from the sun, even beyond the 30 $R_\odot$ limit of the LASCO coronagraph.

These complex type III radio bursts in the frequency range from 1 to 14 MHz can therefore provide the first warning of a CME liftoff on the sun. The study of these low-frequency type III-like bursts, together with the microwave radio observations, will provide new information about the association of CMEs with flares and magnetic reconnection in the corona.

We propose to identify and utilize all the radio signatures associated with a solar-terrestrial event and to relate these to the other solar and interplanetary data described in this proposal, to advance the understanding of the fundamental physical processes involved in the space environment, and to determine how this information can be used to increase the accuracy and reliability of space weather forecasting. Specifically, we will define and establish metrics for using radio emissions to identify and track transient solar-terrestrial events from sun to earth.

## 5. Theoretical/Modeling Tools

### 5.1. Initiation of the CME

Many models focus on the morphology or propagation of Coronal Mass Ejections (CMEs), but very few attempt to explain the exact nature of the mechanism (or mechanisms) that initiates them. What is required is a mechanism that will cause a sudden transition from the pre-onset, quasi-steady state to the post-onset, dynamic state. Many researchers believe that CMEs are produced by a loss of stability or equilibrium of the coronal magnetic field. However, the exact nature of the mechanism which leads to instability or a loss of equilibrium remains controversial. It may be an ideal process like the kink instability, or it may be a resistive one like the tearing-mode instability. Alternatively, it may be a hybrid of ideal and resistive processes.

Terry Forbes, and other members of this MURI team, intend to use numerical methods to analyze the three-dimensional stability of several proposed models which incorporate helical magnetic fields. These models incorporate a field configuration with a curved magnetic flux rope whose ends are anchored in the photosphere. Various researchers have argued that such a rope will become unstable if the number of turns of the field lines within them exceeds a critical value, but there is, as of yet, no rigorous demonstration that this is true. We propose to encode the subroutines which implement the initial and boundary conditions. These initial conditions will be of two types. The first type corresponds to an artificial injection of kinetic energy at the initial time (sometimes referred to as a kinetic driver). The second type is a fully-self-consistent treatment which starts with an equilibrium configuration that is driven to instability by the slow evolution of the photospheric magnetic field.

Wu et al (1995, 1997a,b,c) and Wu and Guo (1997) have developed a self-consistent numerical MHD model to prescribe the initiation of CME and coronal global evolution. Wu is one of the MURI investigators here. With collaborators, he found that the physical source for CMEs was the evacuation of flux-rope from the helmet streamer. The results of the simulations matched with the observations of several CMEs including the 6-10 January 1997 Halo events and 28-29 July 1996 event.

The basic equations for this 3-D axisymmetric model are the equations of mass, momentum, energy conservation and the induction equation in the ideal MHD approximation. The initial state of this model is helical flux-rope in 3-D axisymmetric geometry embedded in the closed field of a helmet streamer. They begin with the construction of a streamer solution using the numerical relaxation (Roach, 1998) method. The next step is to emerge the flux-rope into the closed field region. The solution depends on initial and boundary conditions, which are inferred from observations. Any unstable solution will be used as a warning that a CME may erupt.

Chen (1996) developed a physics-based theoretical model of CMEs and eruptive prominences based on the forces acting on toroidal magnetic flux ropes (Chen 1989). Recent application of the model to observed CMEs has shown that the model solutions can describe the dynamics of observed CMEs within the field of view of the LASCO instrument ($<32\ R_{\odot}$) (Chen et al. 1997, 2000; Wood et al. 1999). The model can be used to describe both the initial rapid acceleration and the subsequent nearly constant-speed phase.

The model starts with an equilibrium flux rope embedded in the corona with density, $n_c$, and overlying magnetic field, $B_c$. The flux rope is then set into motion by increasing the poloidal flux, which is the flux associated with the local azimuthal magnetic field. This process, referred to as “poloidal flux injection,” is different from the more conventional approach in which the photospheric footpoints are quasi-statically sheared. This suggestion is controversial (e.g., Forbes 2000; Klimchuck 2000) but yields testable predictions in terms of photospheric and chromospheric magnetic field vectors. The predictions obtained from the model to date indicate that the poloidal flux injection process should produce subtle photospheric flows at less than the Alfven speed ($\ll 1$ km/s), and changes (10-30%) in the tangential magnetic field over 30-60 min (Chen 1996, 2000), during the early phases of CME eruptions. (The normal component is predicted to remain unchanged.) There has not been any systematic observation to look for such effects. In particular, one needs to check the suggestion that it is the horizontal component that should change in tens of minutes, because that is the component that has not been well-observed at high cadence, to this time.

Note that some attempts have been made to determine the behavior of the tangential field during very impulsive flares (e.g., Wang et al. 1994; Cameron and Sammis 1999). In such cases, a significant component of the tangential field may be aligned with the line of sight. However, the conclusions of these attempts have not been unambiguous because it is not easy to separate the tangential component contribution from other contributions, like seeing, and the decreased signal-noise ratio. Our network of high-resolution vector magnetographs is well-suited to carry out observations of the tangential field in active regions during eruptions. In particular, we will test the suggestion that the tangential magnetic field changes during eruptions, i.e., we will quantitatively test the observational basis for the apparent successes of the model.

One testable prediction is that the acceleration profile, or the height-time profile, and the poloidal flux injection profile have a specific relationship, and that the greater the magnitude and the duration of injection, the greater the acceleration is. The time scale of acceleration is determined by the flux rope magnetic field and the inertia. An interesting and relevant point is that the synthetic coronagraph image of an earth-directed flux rope resembles a halo CME. Thus, the model is able to relate the expansion speed in the solar radial direction to the expansion speeds of the halo projected onto the plane of the sky. All of these quantities can be calculated as a function of the prescribed poloidal flux injection profile. That is, it is possible to compare observed speeds in the plane of the sky and the observed behavior of the tangential magnetic field associated with a CME event, providing a viable test of the flux injection hypothesis.

### 5.2. Interplanetary Propagation of CMEs

To understand the potential geoeffectiveness of a CME, we must understand how the solar wind parameters are modified when the CME passes through interplanetary space to 1 AU. Wu and Guo (1997) extended their model to 220 solar radii. We must determine an undisturbed solar wind solution that is in agreement with the typical observed solar wind parameters at 1 AU. To arrive at this solution, the polytropic index of the energy equqtion is allowed to be a slow function of radial distance in order do mimic the thermal conduction in the solar wind. This extended model has successfully explained the observation of the 6-13 January 1997 CME event (Wu et al., 1999), its propagation in interplanetary space, and its evolution to a magnetic cloud as observed by Wind (Wu et al. 1997b, 1999).

This model could produce the following geoeffective parameters for a given solar disturbance: (i) when and where a shock (or shocks) will form and their strength; (ii) southward IMF's strength as a function of time at 1 A.U. (iii) dynamical pressure as a function at 1A.U. (iv) the solar wind-magnetosphere energy coupling parameters, AE, Ap and Kp indices.

For Chen's model in §5.1, in addition to the study of initiation of CMEs, by continuing the initial-value solutions, it has been shown that the model yields interplanetary flux ropes closely resembling the observed magnetic clouds as the 1 AU counterparts of CMEs (Chen 1996; Chen et al. 1997, 2000). A recent paper (Krall et al. 2000) compared the erupting flux rope model with the set of magnetic clouds observed to date, showing good agreement between the model and observations. Note that the typical calculated propagation time is roughly 80 hours, consistent with many magnetic clouds associated with halo CMEs (Bueckner et al. 1998; Gopalswamy et al. 2000). Evidently, the model can describe the CME/magnetic cloud dynamics quite well.

Furthermore, Chen's model relates the variation in the tangential magnetic field to the eruption speed through the corona to 1 AU (Chen 1996). Thus, if the model is demonstrably correct, it can provide an important tool for relating solar observations of vector magnetic field and photospheric motion to the CME evolution through the interplanetary medium. The model provides the speed, magnetic field strength, and the size of magnetic clouds at 1 AU resulting from CMEs.

Along with the IP propagation of the CME, of course, comes the associated shock, and its acceleration of particles. As shown in Figure 3, the time profile of a SEP can give an indication of the geometry. In §4, we noted that the time-dependent composition and charge-state of accelerated particles can also be referred back to the conditions at the shock. Successfully predicting the onset and development of a SEP event requires a model for the initiation and early development of the shock and the CME that drives it, because the SEPs are created as soon as the shock starts to form. By modeling the formation of the CME and the shock wave, we will be able to estimate the intensity and time evolution of the SEPs, which we plan to do initially using the existing analytic theory of team member Lee (Lee and Ryan 1986). This theory provides a simple prescription for linking the particle spectrum to the strength of the shock wave and its location relative to earth.

Team member Lee will be responsible for the application of the existing theory of diffusive shock acceleration and for the development of a new theory that self-consistently incorporates both acceleration, and transport processes.

## 6. Laboratory Simulations of Eruptive Solar Phenomena

A powerful new technique for investigating the fundamental mechanisms underlying eruptive solar phenomena has recently been developed at Caltech by team member Bellan. This technique uses a pulsed, high power laboratory plasma arranged to have the same boundary conditions as the solar phenomena, and operates in a physics regime governed by the same equations. Because of this equivalence in both physics and geometry, the dynamical behavior and the topological evolution of the lab plasma closely mimics eruptive solar phenomena. Figure 10 shows a typical photo of one of these laboratory plasmas. Since the lab plasma is quite reproducible and can be diagnosed fairly completely, it is possible to make quantitative comparisons with theoretical models and so validate or invalidate these models. It is also possible to reproduce many of the peculiar phenomena seen in observations (e.g., sigmoids (Canfield et al., 1999), filamentation, complex topology) and then study these in a controlled setting. This experiment gives a "hands-on" tool for investigating the underlying topological and dynamical essence of eruptive solar phenomena such as CME's, erupting filaments, and flares.

Fig. 10.— Typical example of laboratory plasma simulating eruptive solar prominence (filament). Distance between footpoints is 8 cm, nominal magnetic field strength is 3-5 kG, plasma current is 30 kA, lifetime is 10 $\mu$s. The plasma $\beta$, topology, and dynamics are similar to what is observed on the sun.

The technique for making these laboratory simulations of coronal structures is sketched in Figure 11. A magnetic bipole (horseshoe magnet) mounted on the wall of a large vacuum chamber creates an initial quasi-stationary, arch-shaped, potential magnetic field of a few kilogauss which protrudes into the vacuum chamber. A plasma is formed via electrical discharge in the region between the magnet poles and then a current is driven from one magnet pole to the other by a high energy capacitor bank. Initially, when the current is small, it simply follows the arched potential field lines [cf. Figure 11(b)], but as it increases to 10's of kiloamps, it self-pinches, causing its cross-section to become uniform along its length, just like an erupting solar filament. The self-field also causes the current channel to twist and writhe [cf. Figure 11(c)], again like a solar filament. Finally, for very large currents, the upward current on one leg of the prominence and the downward current on the other leg mutually repel leading to a bulging of the major radius of the current channel [cf. Figure 11(d)]. This bulging stretches the original potential field and, if sufficiently strong, leads to eruption.

Besides manifesting the fundamental magnetohydrodynamic forces believed to govern eruptive solar phenomena, the experiments so far have reproduced many important details. In particular, the lab plasmas display sigmoidal shapes (when viewed from above), and develop smaller braided filamentary structures which are both twisted and interwoven. The most recent set of experiments has demonstrated that an over-arching arcade field can inhibit eruption, and quantitative measurements indicate that the required strength of this larger scale arcade field is in good agreement with the predictions of a three-dimensional MHD force-balance model.

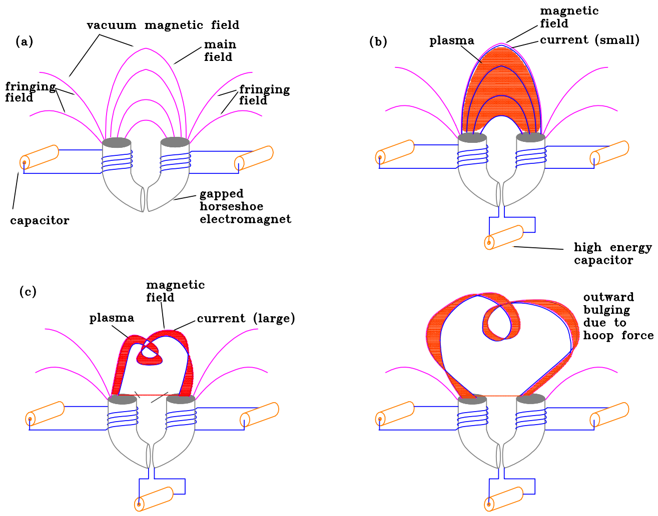


Fig. 11.— Experimental method: (a) initial vacuum field from gapped horseshoe magnet, (b) small plasma current follows initial arched field lines, (c) large plasma curent causes field lines to pinch and twist, (d) very large current causes arched field lines to bulge outwards.

## 7. Expected Products

### 7.1. Initiation and Propagation of CMEs

From our observations and theoretical models, we will pin down the conditions for the initiation of CMEs: the magnetic topology and solar surface manifestation.

There are several models that have been put forward to describe the process from filament eruption to the eventual geomagnetic storms. In a recent study given by Wu et al (2000), they used LASCO/EIT/SOHO observations and a simulation model (Wu and Guo, 1997) to reveal three distinct physical processes of CME initiation: (i) filament eruption, (ii) photospheric shear and induced loss-of-equilibrium of a helmet streamer and (iii) plasma flow resulting from chromospheric evaporation. They further suggested that a CME generated by a filament eruption is faster than one generated by shear-induced loss of equilibrium. In addition, there is a new

3-D MHD model (Wu et al. 2000) to simulate the observed EIT waves which could be used for CME initiation study. This new MHD model will be used to study EFR initiated CMEs. The results of these models can be tested by our observations.

Forbes will test the initiation of CMEs using two types of initial conditions. The first type corresponds to the artificial injection of kinetic energy at the initial time. The second type is a fully self- consistent treatment which starts with an equilibrium configuration that is driven to instability by the slow evolution of the photospheric magnetic field.

As part of the effort to observationally investigate possible initiation mechanisms, we will also examine the photospheric flows and changes in the normal, as well as tangential magnetic field. The most widely held "paradigm" of solar eruptions is that the magnetic field footpoints in the photosphere are slowly sheared. This approach has been used by one of our MURI members, Forbes, in modeling initiation of flux ropes. The work to date has been based on hypothesizing specific flow patterns, and seeking some catastrophic loss of equilibrium or stability. However, no particular shear flows have been directly related to an observed eruption. Clearly, if photospheric flow patterns can be quantitatively related to eruptive behaviors, the resulting understanding will advance the ability to predict the terrestrial consequences of solar eruptions. In this MURI, we will attempt to derive more quantitative flow signatures associated with eruptions. Dr. Chen will further develop his model of a flux rope leg embedded in a highly stratified plasma medium to investigate the process of azimuthal magnetic field propagation though the photosphere and the chromosphere. For this purpose, he will construct both theoretical and MHD simulation models. He has initiated a number of studies in an attempt to address some basic issues concerning magnetic field transport through a highly stratified medium (Huba and Chen 1996; Krall et al. 1998). These studies were limited in scope, but Dr. Chen will build on these studies. Furthermore, Dr. Forbes and Dr. Wu are both experts in MHD simulations of solar phenomena. For the MURI, Drs. Chen, Forbes, and Wu will work closely together to address questions concerning the CME initiation process, and develop testable signatures of the proposed mechanisms. In this regard, these members of the MURI represent diverse points of view. The specific tasks to be proposed in this MURI will be discussed later.

Wu, Forbes and Chen will work closely, and work on the following specific issues to be investigated:

(1) Develop a model of poloidal flux injection through the photosphere and obtain testable signatures in terms of the vector magnetic field and the 3-D photospheric flows (i.e., including the vertical component). These quantities are detectable using the vector magnetographs in our network and Doppler measurements. The expected values, based on the initial estimates, are 10-20 G in the tangential field near the photospheric footpoints and 1 km/s, changing on a time scale of tens of minutes.

(2) Develop a model of halo CMEs. In conjunction with the above task, determine the projected speed of a halo CME in terms of the vector magnetic field variations in the photosphere. Predict the transit time to 1 AU, the magnetic field strength, and the size of magnetic cloud in terms of the variation in the tangential magnetic field.

The erupting flux rope model includes a model corona and a model solar wind (Chen 1996). Consider the scenario where a flux rope interacts with slower/faster solar wind as it propagates to 1 AU. Theoretically, it was predicted that the range of CME speeds should decrease with heliocentric distance. This conclusion is based on a model of momentum coupling between a flux rope and the ambient solar wind via a drag term. The drag coefficient was estimated using an MHD simulation study of flux rope-solar wind interaction (Cargill et al. 1996). Recently, the range of observed CME speeds near the sun has been shown to be greater than that of observed interplanetary magnetic clouds (Gopalswamy et al. 2000). By comparing the observed variation in the (statistical) range of CME/magnetic cloud speeds with the predicted variation, we will test the momentum coupling process modeled by theory and simulations.

(3) Extend the earlier work of Cargill et al. (1996) to include nonuniformity in the ambient solar wind. Investigate MHD shock generation by magnetic flux ropes. The deformation of flux ropes in interplanetary space will also be investigated as a function of density and speed of the flux rope in relation to the ambient solar wind density, speed, and magnetic field.

We emphasize that it is not a primary objective under the proposed MURI to use the erupting flux rope model of Chen (1996) as a tool to predict propagation of CMEs to the earth. This is because although the model results appear to be in general agreement with observations of CMEs and magnetic clouds, the interplanetary medium through which a CME propagates is not well-known at any given time. Rather, the objective here is to understand the physical process of CME eruption and propagation better by bringing together a critical mass of the latest observational tools and theoretical/simulation ideas and critically examine/test a diverse range of ideas. The main themes in this respect are to understand the relationship between observable solar disk phenomena (e.g., EIT waves, EIT and X-ray dimmings, vector magnetogram measurements) and earth-directed CME dynamics. Fundamentally, we seek to develop a quantitative model to relate the magnetic field strength, polarity, and the speed of magnetic clouds at 1 AU to observable solar quantities (e.g., those mentioned above). The flux rope model is potentially applicable to magnetic clouds as 1 AU counterparts of CMEs. Magnetic clouds are estimated to constitute approximately 1/3 (Gosling 1990) or more (Webb et al. 2000) of CMEs.

The model output for CMEs near the sun consists of the height-time curves for the leading and trailing edges and the aspect ratio, which is the ratio of the height of a CME to its transverse width. The above quantities are directly comparable to coronagraph data, if the eruption is from the disk center. The test of such a model requires an accurate determination of the onset of eruption. Continuous H$\alpha$ monitoring at our three stations will provide an ideal setup to obtain the onset time and location of an eruption that causes a CME. We will identify the times of surface eruptions and corresponding magnetic disturbances at 1AU to test the CME speed predicted from Chen's model as well as the streamer and flux-rope interaction model (Wu et al., 1999).

### 7.2. Monitoring Emerging Flux Regions (EFRs), Flares, Filament Eruptions, and Radio Bursts

EFRs have two known effects in triggering solar activity. Tang and Wang (1993) found that major flares tend to be associated with new flux emergence. Feynman and Martin (1995) found that filament eruptions are likely to be triggered by EFRs. The underlying physics for these two observations is straightforward – an equilibrium magnetic configuration can be sharply perturbed by new flux emergence. So, monitoring of new flux emergence is very important in tracking solar activity. EFRs can be monitored by full-disk magnetograms; however, our full-disk H$\alpha$ network observations will be able to provide good detection, based on the appearance of arch-filament systems. Based on our experience, arch-filaments and the brightenings associated with them, appear even before new spots are noticed in the magnetograms. EFRs will be reported on our web site in real-time. SOHO/MDI and GONG full-disk magnetograph data will be used to confirm the new flux emergences. BBSO is the mainland US GONG site in that six-station network.

Flares and filament disappearances can occur anywhere, and at any time, on the solar disk. High resolution, high cadence solar images with 24-hour coverage will certainly be essential to catch all flares on the visible disk of the sun. High spatial resolution and cadence will also allow a detailed description of the evolution of flares, as well as their associated active region(s). This is the core scientific objective of our H$\alpha$ network. This proposal also includes a radio network component, both to relate the H$\alpha$ activity with the presence of energetic particles, and to ensure that all events will be detected, even when they would otherwise be missed due to clouds.

The various and diverse radio signatures provide remote sensing tools for specifying and forecasting the space environment associated with solar eruptive events that have significant geophysical consequences. The complete radio frequency coverage from 20 kHz to 18 GHz provided by this MURI collaboration will provide a means of better identifying and understanding solar eruptive events and the acceleration of particles in the corona and their associations with coronal shocks and flares. It is anticipated that these comprehensive radio observations will improve our ability to understand, predict, and quantify SEP events.

Until now, H$\alpha$ full-disk images depicting solar flares were normally saturated because the exposure time was set to a constant value for the typical 8 bit dynamic range camera, and optimized to yield high contrast images of the quiet sun. The bright flaring regions were therefore over-exposed. Since the H$\alpha$ intensity gives a minimum temperature for the flaring region, it is important to obtain proper photometric data, especially when the full-disk brightness is suddenly rising during a flare. While two of the cameras in our network have a 14 bit dynamic range, one has only an 8 bit range. But an automatic software control has been implemented in that camera's control software, changing cadence and exposure time, which permits an accurate evaluation of flare brightness even with that camera. This significantly improves the photometric measurements. To demonstrate the capability of flare monitoring at 8 bits, the temporal evolution of an M7 flare is shown in Figure 12 during its maximum phase from 16:31 to 16:51 UT on 29 April 1998.

We anticipate that the duty cycle of our H$\alpha$ network will be over 80%, so that most flares and filament disappearances on the disk will be detected by our automatic program. Their time of occurrence, location and size will be posted on the web page in real-time. The software for this is almost complete. Associated radio emission parameters (peak frequency, peak flux, duration, spectral slopes) will also be posted from the radio network. For those events that are missed in H$\alpha$ due to clouds, or even events beyond the solar limb, the radio emission parameters will be available. *Combined, these two ground-based monitoring systems will provide the most complete coverage of solar events ever obtained.*

To establish metrics for forecasting geoeffective space weather events from solar observations, it is essential to be able to accurately identify their solar origin, which can occur anytime from 1 to 4 days before the terrestrial

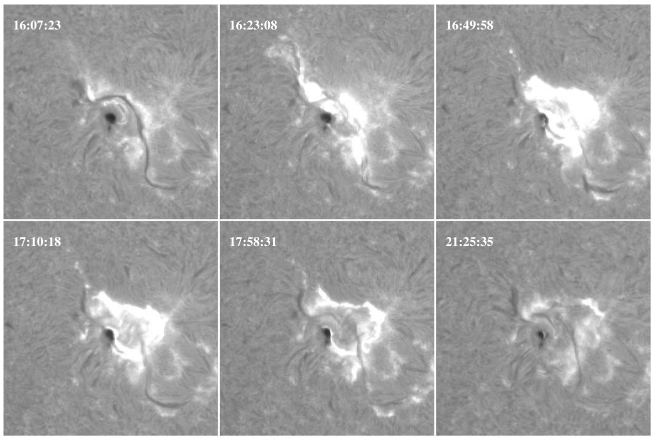


Fig. 12.— Temporal evolution of an M7 flare and eruption of a filament in the active region NOAA 8210 observed on 29 April 1998. The field of view of the individual frames amounts to $400'' \times 400''$. The images are from BBSO full-disk data.

manifestation of a space weather event. This becomes more difficult during solar maximum when there can be several major eruptive solar events per day. The complete radio coverage (space and ground-based) provided by this MURI collaboration, which provides the intermediate link between the solar and terrestrial space weather event, will play an important role in establishing the solar origin because the radio observations provide a global view of the entire solar-terrestrial event which can therefore uniquely connect a space weather event with a solar event.

### 7.3. Statistical Studies of Eruptive Filaments, Flares, CMEs, Magnetic Clouds, Particle Events and Geomagnetic Disturbances

A key component of this proposal is to monitor the propagation of CMEs and associated phenomena, from initiation at the sun to 1 AU, and their effect on the magnetosphere. We understand that the ultimate goal of space weather prediction is to predict geomagnetic disturbances at or near 1 AU. This is the most difficult part. We propose to carry out statistical correlation studies to better understand the physical connections between solar surface activity and geomagnetic disturbances, to enhance our ability to predict geomagnetic disturbances, and place upper limits on their intensities.

Large geomagnetic storms are usually caused by a structure in the solar wind having a specific feature – a long duration of strong southward interplanetary magnetic fields (IMF), impinging on the earth's magnetosphere. There are two possible stages at which to monitor geomagnetic storms: (1) to observe magnetic field fluctuations by a satellite, such as ACE or Wind. This may give a few hours of advance warning as the disturbance travels from the satellite to earth. However, the prediction is still not very certain. (2) to measure the Dst index (the degree of equatorial magnetic field deviation, by ground stations). This gives a "nowcast", and perhaps some advance warning through forward projection of the Dst profile as it develops (e.g. Klimas et al. 1997,1998; O'Brien & McPherron 2000), incorporating real-time ACE solar wind data.

Our objective here is to obtain as much as 2-3 days advanced warning, from statistical results on filament eruptions and geomagnetic disturbances based on hundreds of events. A correlation between filament eruptions and magnetic clouds has been suggested (e.g. Bothmer and Schwenn, 1994; Burlaga et al., 1997; Wilson and Hildner, 1986; Marubashi, 1997). In particular, Marubashi (1997) found a good correlation between the structure of erupted solar filaments and the structure of interplanetary magnetic clouds. With a much improved data base, we will search for possible relationships between filament eruptions and geomagnetic disturbances reported by ACE and Wind in the form of in situ magnetic field fluctuations. We will also directly study filament eruptions and the Dst index. We plan to plot the Dst index, the Bx, By and Bz (in situ magnetic field components measured by Wind and ACE) as a function of time, then mark the filament eruption events in the curves. We are especially interested in the time delay between solar surface phenomenon and geomagnetic disturbances. This delay will be tabulated for statistical study. Quantitative correlation coefficients will be established to aid future forecasts. In particular, we will evaluate and perhaps refine the empirical relationship between CME speed at the sun and its arrival time at 1 AU, as given by Gopalswamy, Lara and Kaiser (2000).

If the Gopalswamy et al. relationship holds, it means the initial speed of earth-directed CMEs (an important quantity that is hard to measure with LASCO due to the occulting disk) can be determined from the arrival time at 1 AU. CME speeds in turn should be related to shock strength, and hence the flux and duration of SEP events versus shock strength can be studied for a large number of events. Correlations with type II shock speed, magnetic configuration, and other parameters promise to result in better predictive measures.

CMEs will be tracked through their associated radio emission, from the solar corona out to 1 AU by making use of the fact that as shocks propagate through the corona and interplanetary medium they generate radio emissions at lower and lower radio frequencies. These measurements will enable us to study and quantyfy the CME dynamics, including possible acceleration or deceleration. These observations will be used to more accurately 'redict the arrival times of CME events at 1 AU.

The mere occurrence of an event on the sun is insufficient for a warning, however. We must be able to distinguish geoeffective events from non-geoeffective ones. To do this, we will compare the magnetic topology of the filaments and overlying arcade structure with magnetic cloud structure, as demonstrated in Figure 13 for the February 17, 2000 event. For this particular event, a clear halo CME was created, and a substantial magnetic cloud was detected by ACE, however, there was no geomagnetic storm associated. We found that the reason is that the orientation of the cloud magnetic field was northward. This orientation is consistent with that of the field orientation of the erupting filament. Therefore, it is important to monitor the pre-eruption magnetic configuration, in order to measure the filament field direction, and hence the geoeffectiveness of the CME after the filament/flare event occurs. Figure 13 also shows the magnetic vector of magnetic clouds as measured by the magnetometer on board ACE on February 21, 2000. Figure 14 compares the orientation of magnetic clouds, solar surface magnetic fields derived by force-free extrapolation, filament direction and earth's magnetic fields. It is reasonable to conclude that the field orientation that the structure has at the solar surface does not change during propagation in interplanetary space. Therefore, after analyzing a large number of events, it may well turn out that we can use the surface magnetic orientation as a proxy to predict the geoeffectiveness of the erupting events - implying a *new*, more precise early warning of geoeffectiveness.

We will use any statistical relationships we discover among the various solar and IP measurements to help predict the occurrence of SEP events at the outset of an event. In addition, during propagation of the CME and its associated IP shock, we will monitor the time profile of energetic particles (for those with an associated SEP event), to refine the location of the shock relative to earth, and its connectivity with spacecraft at various points in the heliosphere, as shown in Fig. 3. This information can be used as a check on the models, to update the prediction of geoeffectiveness as the event progresses.

### 7.4. Quantitative Flare, CME, and SEP Prediction Parameters

Although flares are not an absolute indicator of geoeffective CMEs, many large flares have major consequences for space weather. Predicting them is very important. It is important to point out that flares occur in a localized region (active region) while CMEs are related to global structures, such as helmet steamers. The energy source for both phenomena is magnetic. To accurately predict solar flares and CMEs, some quantitative

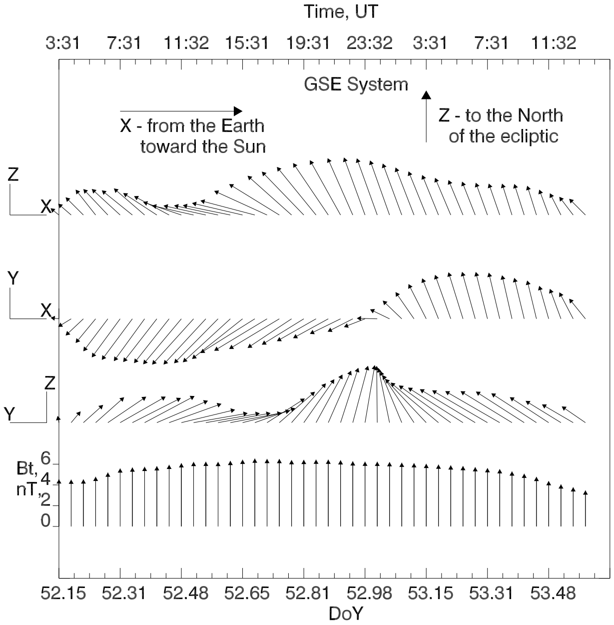


Fig. 13.— ACE measurement of magnetic fields in the magnetic cloud of February 21, 2000, which was the result of the halo CME on February 17.

parameters need to be established in order to understand flares better, and to make more objective predictions.

We will provide quantitative parameters to elucidate the non-potential properties of active regions. Based on analyses of vector magnetograms, one may establish several parameters to describe the degree of deviation from a pure potential field which is the minimum energy configuration. Initially, we plan to use two parameters, integrated magnetic shear and integrated vertical electric currents, as the indices for flare prediction. Some other parameters may be used when we have a better under-

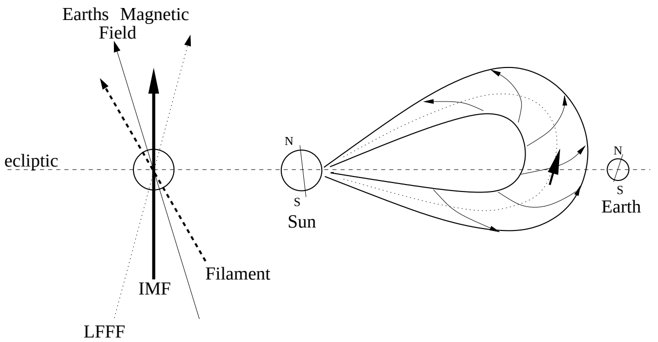


Fig. 14.— Comparison of the orientation of a magnetic cloud at 1AU, the magnetic fields derived by linear force-free extrapolation, the filament orientation and earth's magnetic field.

standing of magnetic structures and their parameters. Although a relationship between "magnetic shear" and the onset of flares has been somewhat established (Hagyard et al. 1984, 1990; Falconer 1999), a quantitative description of such a relationship and the forecasting parameters need to be established based on a much larger number of events which will be observed by our vector magnetograph network. Specific quantitative shear in relation to CME initiation has been investigated observationally, but modeling effort is being carried out (Wu et al., 2000)

(1) Integrated Shear

The term "magnetic shear" was first introduced by the NASA/MSFC group, when they found that the shear angle (the angle between the observed field vector and the potential field calculated from the longitudinal field), the transverse field strength and the length of the sheared neutral lines are closely associated with the probability of flares. We expect a similar study will be extended to CME.

At BBSO, we defined the new term "shear" as the product of the shear angle and the measured transverse field strength (Wang, 1992). This term was introduced to describe the magnetic shear in active regions. We introduced this new definition of shear, instead of the pure shear angle defined by Hagyard et al. (1984, 1990), because (1) the strong transverse field regions contribute more significantly to the free magnetic energy of shear, and (2) the measurement errors in the azimuthal angles for strong field regions are significantly reduced. Since every point has a well-defined magnetic shear, two dimensional shear maps can be constructed. A time sequence of shear maps will be compiled to visualize the development of magnetic shear. Such data sets have been made and studied for several flares (Wang, 1992). The shear integrated over some particular active region will be called "integrated shear". We will monitor this shear parameter for each active region and set a threshold for triggering a warning of possible, impending major flares.

(2) Integrated Vertical Currents

The vertical current density is calculated by

$$J_z = \frac{dB_y}{dx} - \frac{dB_x}{dy}, \tag{3}$$

which is another important way to quantitatively describe the degree of non-potentiality in an active region. Since only one layer of the magnetic field can be obtained, only the vertical component of the electric current can be derived directly. The analyses of vector magnetograph data from the Mees Solar Observatory (MSO) yielded important results about the relationship between the vertical currents and electron precipitation of flares (Canfield et al., 1993; Leka et al., 1993). They found that the precipitation of electrons is concentrated at the borders of strong, vertical current regions – the two sites are not co-spatial. At BBSO, Li et al. (2000) found an important link between the occurrence of major flares and the appearance of new currents brought up by flux emergence. More recently, Falconer (2000) found a close connection between the occurrence of major flares and net currents, and the length of the sheared neutral line in active regions. We will do real-time monitoring of the integrated net and total current in active regions, and establish a threshold that will trigger the warnings of solar flares.

Our shear and current curves will be updated hourly when one of the stations in our network is observing, and will be posted on the BBSO web site. When we are following particularly interesting regions, these curves will be updated every few minutes. We only need to transmit calculated parameters to BBSO from the two stations. At this time, we do not have an exact projection about the threshold values for triggering a warning. As this project progresses, many events will be observed and studied, and reasonable thresholds will be set based on the statistical results.

The magnetograms obtained from our IR system will help the calibration of our visible system, and will produce more accurate measurements with lower cadence. The more accurate magnetograms will be critical in constructing current and shear maps.

Relating such solar surface measures to the prediction of SEP events is more speculative, and depends on what we find in correlative studies. If we find that SEP events require a pre-existing population of seed particles, for example, we can use the radio monitor data to identify when conditions for shear or coronal currents occur together with pre-existing fast particles. That is, a region with frequent flaring that also contains a lot of shear might be more likely to produce a SEP event, and furthermore the likelihood may drop as the time since the last flare grows. We will search for evidence of such correlations, and if found, use them to define quantitative prediction measures.

Based on our observations and real-time monitoring of solar magnetic fields and activity, we propose to develop an improved activity report and warning system.

Certain parameters are necessary to carry out the predictions. The primary input is very good records of the sun – high-resolution images which show the configuration of the magnetic field, and the existence of stressed fields which appear to be closely connected to the occurrence of flares. Once one observes stressed fields, it is a fairly easy matter to predict flares and to issue warnings. However, the warnings have only a one- or two-day horizon, since we cannot predict the time at which a flare will occur. We believe the best, and most important, direction for investigation is to study the emerging flux regions and develop criteria for whether or not they will grow to great size, or to the level of complexity which will produce flares. This will lead to longer term and more accurate forecasts.

The improved program will have quantitative parameters to guide us, while we will also rely on our experience. In addition, we will have staff members on duty 24 hours. For this, we have a commitment from HSO, YAO, KSO and IAC. They will use the H$\alpha$ and magnetograph data obtained on-site to guide forecasting. Each of the five stations will issue an activity report once a day. If we believe that a major event is imminent, any station will issue a warning by e-mail during its local day time.

We have extensive experience in flare predictions. Our predictions (BBSO Activity Reports and Warnings) have achieved an accuracy of about 90%. However, the main task in this proposed research is to predict geoeffective events. Based on our observation and models, we will predict the geoeffectiveness, in addition to the possibility of occurrence of events.

(3) Multivariate Discriminant Analyis

Vector magnetograms will be used to derive a number of objective parameters relating to preflare conditions. In particular, line integrals of magnetic shear weighted by field strength, gradients, lengths, flux emergence rates, and neutral line curvature will be used in a statistics package that relates these parameters to subsequent flare rates and magnitudes. The use of Multivariate Discriminant Analysis (MVDA) (e.g. Neidig et al. 1981) was previously applied to a limited set of vector magnetic field data in an attempt to develop an objective algorithm for flare prediction (Smith et al. 1996). While the results of this study on 57 active regions showed a clear, prediction-effective relationship between magnetic shear and flare activity, the data base was nevertheless too small to establish the relationship with large, geoeffective events. The much larger and more consistent data base made possible under the current proposal will allow the derivation of an improved MVDA-based algorithm. This algorithm will then be applied and tested on an independent sample that includes large, geoeffective events.

Since we will develop quantitative prediction parameters, which has not been done before, our automated predictions will be much more prompt and accurate than any current predictive method.

### 7.5. Comparison with Laboratory Results

Both theories of eruptive solar phenomena and the laboratory experiments show that the behavior of complex coronal structures such as CME's, flares, and filaments is primarily determined by two independent types of boundary conditions on the solar surface, namely (i) the magnetic field normal to the surface $\mathbf{B}_n$ and (ii) the plasma velocity tangential to the surface, $\mathbf{U}_{\tan}$. By itself, the normal magnetic field produces static, arched potential fields. The addition of cyclonic tangential velocities twists up these arched fields leading to bulging, sigmoidal shapes, and finally eruption. Both the normal magnetic field and the tangential plasma velocity are independently adjustable in the lab experiment. The normal field can be adjusted by using different electromagnet arrangements (e.g., four magnet poles instead of two, different spacings between poles, different symmetries, strengths, geometrical extents, or complexities). The tangential plasma velocity can be adjusted by changing the surface distribution of the electrostatic potential $\phi(x,y)$ imposed by the capacitor bank. This is because the tangential velocity at the surface is just $\mathbf{U}_{\tan} = -\nabla\phi(x,y) \times \mathbf{B}_n(x,y)/B_n^2$ , so that local maxima or minima of potential (such as are produced by electrodes) create cyclonic plasma velocities in the plane of the surface. The effect of changing the normal magnetic field has been clearly demonstrated by using several different magnet configurations. Control of the tangential velocity $\mathbf{U}_{\tan}(x,y)$ has also been demonstrated by using different shapes of ground plane electrodes (solar surface). The chirality (handedness) of the twist has been changed by reversing the polarity of $\mathbf{B}_n$.

Systematic studies of various topological configurations will be undertaken and the relationship of topology to eruption will be elucidated. Erupting filaments have been produced in the experiments to date. By careful control of the surface velocity shear profile, it is planned to reproduce the more complicated situation of a CME overlying a filament. Precursors for eruption will be examined, for example the degree of sigmoidal behavior prior to an eruption.

The experiments have also shown that the visual appearance of a simulated prominence (filament) depends strongly on the angle from which it is viewed. This is because, as with solar plasmas, the simulated prominence is optically thin and so the optical depth of what is being viewed strongly affects the observed brightness and hence the perceived image. This important perception issue will be investigated in detail by photographing various structures from different points of view and by making 3D images using an existing high-speed stereo camera system.

As an additional part of this activity, the lab plasma setup will be upgraded to produce a direct simulation of the sun-earth connection. An expanding, propagating lab prominence will play the role of a helicity-laden magnetic cloud propagating through interplanetary space.

By placing a small dipole magnet in the path of the expanding helical flux tube, a situation analogous to the sun-earth connection will be established. The interaction between the large propagating helical field and the much smaller static dipole field will be studied. This experiment will show how magnetic clouds shed from the sun by an eruptive solar event affect earth's magnetosphere.

The lab experiments will be both highly visual and quantitative, and so will have a strong connection to both solar observations and the various theoretical models attempting to describe these observations. The experiments are expected to provide compelling, quantitative insight into the fundamental physics governing CME's and filament eruptions and also the topological issues relating to these phenomena.

## 8. Implementation Plan

### 8.1. Science Team

Table 2 shows the team members, their institutions, and a brief statement of their areas of expertise or roles on the team. The number in the first column of Table 2 is used in Table 3 to further identify each team member's role in the project.

Phil Goode is the PI of this proposal. He holds the rank of Distinguished Professor in the physics department of NJIT, and is the director of BBSO. He has a strong record in solar physics research. He currently has annual funding of about $800K to support the operation of BBSO, mainly from NASA and NSF.

The row headings in Table 3 are taken directly from the National Space Weather Program (NSWP) Implementation Plan. Our plan is closely aligned with the NSWP, and can be considered a subset of this much larger program. Our program is fully consistent and supportive of NASA's Living With a Star (LWS) initiative. In keeping with our understanding of the goals listed in the description of this MURI Space Weather topic, our plan emphasizes the solar and heliospheric components of Space Weather, and uses space- and ground-based magnetospheric measurements as "ground truth" indicators of the success of our predictions.

In addition to the team members identified in Table 1, we also have international partners at various optical and radio observatories around the world. Our current partners who are part of the NJIT H$\alpha$ Network include Kanzelhohe Solar Observatory in Austria, IAC in the Canary Islands, and Beijing and Yunnan Observatories in China. Other partners for radio sites are Observatoire de Paris, (Meudon/Nancay), and the Korean National Radio Observatory.

We have formed an external advisory committee to provide oversight for our proposed project. The current members are Dr. Art Poland NASA/GSFC, Dr. Ernest H. Hildner, NOAA and Dr. B.C. Low, HAO. The committee will participate in our yearly workshops, and will critique our plans each year for the following year's efforts, to ensure that we stay on track and on schedule.

### 8.2. Yearly Milestones

In addition to frequent email and telephone contact among participants, we also plan yearly, detailed scientific workshops, so that members of the team can maintain a tight cooperation which is essential to success in this team effort. In the workshop, members will focus on selected space weather events. In this, we will use combined data, and synthesize the models to determine a complete picture of events and use the results as tools for prediction. Both BBSO and NJIT have video conferencing centers, which also will be utilized for effective communication.

The are two parts to our proposed product. First, published scientific papers reporting results which enable us to understand the physics of space weather. Second, advanced forecasting tools and results available in real-time on our website.

#### *8.2.1. Year 1*

Early in the first year, we will hold our first workshop to bring all team members up to speed on relevant activities each institution has done or is planning. Then, we will coordinate the various joint activities of the team members. The optical, radio and laboratory hardware component of the proposal, if funded, will be completed by the end of this first year, so that 24-hour coverage can commence as quickly as possible. We will also begin continuous monitoring with existing facilities, and set up a project file- and WWW-server that will maintain the latest data and results, as well as archives of the monitor-data products. We will begin broad case studies of some recent events, coordinated across institutions, in order to test observational or derived quantities for their value in event prediction. We will gather data during this period for statistical studies of correlation among phenomena. All our real-time space weather forecasting will be available on our website. As our products are improved, the improvements will be reflected in what we report on our website.

#### *8.2.2. Year 2*

The observing network should be complete early in the second year, and real-time operational data will be monitored on the web server to alert relevant team members of activity. We will continue with case studies, and will begin to synthesize models (e.g. Chen, Wu,

Table 2
Science Team

| Team # | Name | Institution | Position | Role/Expertise |
|---|---|---|---|---|
| 1 | Philip Goode | NJIT/BBSO | Distinguished Professor Director, BBSO | Operate H$\alpha$, magnetogram network |
| 1 | Haimin Wang | NJIT/BBSO | Professor Assoc. Director, BBSO | Operate H$\alpha$, magnetogram network |
| 2 | Dale Gary | NJIT/OVSA | Assoc. Professor Director, OVSA | Operate SRSP network |
| 3 | Paul M. Bellan | Caltech | Professor | Erupting filament laboratory expt. |
| 4 | Terry Forbes | UNH | Research Professor | Solar MHD theory/modeling of CMEs and eruptions |
| 4 | Martin Lee | UNH | Professor | IP Shock particle acceleration theory |
| 5 | Mukul Kundu | UMd | Professor | Solar $\mu$-wave and m-wave radio obs/interpretation |
| 5 | Stephen White | UMd | Associate Research Scientist | Solar $\mu$-wave and m-wave radio obs/interpretation |
| 6 | S.T. Wu | UAH | Distinguished Professor | MHD theory, modeling of CMEs and solar wind |
| 7 | Thomas Zurbuchen | UMich | Assistant Research Scientist | Operate spacecraft data center, particle/SW comp |
| 8 | Donald Neidig | NSO/AFRL | Principle Astrophysicist | Space Weather/ISOON Network |
| 9 | James Chen | NRL | Research Physicist | CME/magnetic cloud models and magnetosphere interaction |
| 10 | Simon Plunkett | NRL | Assoc. Research Scientist | LASCO CME observations, STEREO coronagraph |
| 11 | Louis Lanzerotti | Bell Labs/LT | Distinguished Member of Technical Staff | Multi-spacecraft IP particle obs, and polar magnetographs |
| 12 | Michael Reiner | Raytheon/GSFC/ Catholic U. | Chief Scientist | Wind IP radio observations STEREO radio experiment |
| 13 | Bernard Blake | Aerospace Corp | Research Scientist | Particle and field effects within magnetosphere |

TABLE 3
ROLE OF SCIENCE TEAM MEMBERS BY TOPIC*

| | Physical Understanding | Model Development | Observing Systems | Education |
|---|---|---|---|---|
| Coronal mass ejections | 1-6,9,12 | 4,6,9 | 1,2,5,10,12 | 1,2,3,5,6 |
| Solar activity/flares | 1-3,5,6,8,9 | 3,4,9 | 1,2,5,8 | 1-5 |
| Solar Energetic particles | 2,4,5,7,11,12 | 2,4,7 | 2,5,7,11 | 2,4,5,7 |
| Solar UV/EUV/soft x-rays | 1,2,5,10 | — | 1,2,5,10 | 1,2,5 |
| Solar radio noise | 2,5,11,12 | 2,11 | 2,5,11,12 | 2,5 |
| Solar wind | 4,7,9,11 | 4,6,9 | 7,11 | 7 |
| Magnetospheric particles and fields | 4,11,13 | 4,11 | 11,13 | 4 |
| Geomagnetic disturbances | 6,9,11,13 | 11 | 11 | 6 |
| Radiation belts | 2,5,11,13 | 13 | 13 | — |

*See Table 2 for Participant Key

Forbes, and Lee) into a single framework. We will begin the correlative studies of observed phenomena. We will experiment with the production of daily space weather maps showing schematically the best guess for the location of CME's and shocks, similar to earth weather fronts. These will be initially based on CME location, extent, and speed, propagated forward in time based on IP conditions and model predictions, updated by particle measurements.

#### *8.2.3. Year 3*

We will continue the statistical studies, refining the correlations as we add more data. We will begin to make and test actual predictions in real-time, including real-time modeling, similar to the predictive model of team member Chen. We will follow events in real-time from the sun, through IP space (through radio and in situ particle measurements), to their arrival at L1, and finally to their interaction with the magnetosphere. We will use the magnetometers and the spacecraft measurements within the magnetosphere to relate the severity of the event to the parameters initially predicted and as observed at L1.

#### *8.2.4. Years 4 and 5*

If we continue the program into years 4 and 5, we expect to continue the statistical studies and do more comprehensive case studies based on our real-time monitoring experiences. We will use what we learn from these studies to create and utilize second generation predictive tools. Our improved physical understanding of geoeffective events from sun to earth will set the stage for new discoveries from the STEREO and Solar-B missions, which should be coming on-line at that time.

### 8.3. Education

We include six Ph.D. students in this proposal, three from the base budget, and three from the MURI fellow option. Our team members have excellent records in training Ph.D. students. In particular, NJIT currently has 9 Ph.D. students in solar physics. We believe that this MURI would provide an excellent opportunity to train members of the next generation of solar physicists, including those who are experts in space weather and the forecasting of it. Students will be involved in instrument setup, observations, data analyses and modeling work. Since this is a big consortium, the education of the students will be enhanced by working with faculty members from the various universities and other partners. This will be focussed by their participation in our annual workshop. In addition, this proposed project will train 7 post-docs.

### 8.4. Sub-Awards

The proposed budget includes subaward to 5 universities.

- Sub-award to University of Maryland will support a post-doc and a Ph.D. student, to work with White and Kundu.
- Sub-award to University of Alabama will support 5% salary of Prof. S.T. Wu, a post-doc and a Ph.D. student working with him.

- Sub-award to University of New Hampshire will support 3 months effort of Forbes and 2 Month's effort of Lee.
- Sub-award to Caltech will support a post-doc working with Bellan on the laboratory experiment.
- Sub-award to University of Michigan will support 1/3 of Zurbuchen's time.

## 9. BIBLIOGRAPHY


Ai, G., 1987, Pub. Beijing Astro. Obs., **9**, 27

Bothmer, V. and Schwenn, R., 1994, Space Science Reviews, **70**, 215

Bougeret, J.-L. et al., 1995, Space Sci. Rev., **71**, 231

Bougeret, J.-L. et al., 1998, GRL, **25**, 2513

Brueckner, G.E. and 14 others, 1995, Solar Physics, **162**, 357

Brueckner, G. E., Delaboudiniere, J.-P., Howard, R. A., Paswaters, S. E., St. Cyr, O. C., Schwenn, R., Lamy, P., Simnett, G. M., Thompson, B. and Wang, D., 1998, GRL, **25**, 3019

Burlaga, L.F. and 11 others, 1997, JGR, **103**, 277

Cameron, R. and Sammis, I, 1999, ApJ Letters, **525**, L61

Cane, H.V. and Reames, D.V. 1988, ApJ, **325**, 895

Cane, H. V., R. G. Stone, J. Fainberg, R. T. Stewart, J. L. Steinberg and S. Hoang, 1981, GRL **12**, 1285

Cane, H. V., Sheeley, N.R. Jr. and Howard, R.A. 1987, JGR **92**, 9869

Canfield, R.C., Delabeaujaudiere, J.F., Fan, Y.H., Leka, K.D., McClymont, A.N., Metcalf, T.R., Mickey, D.L. and Wulser, J.P., 1993, Ap.J., **411**, 362

Canfield, R.C., Hudson, H.S. and McKenzie, D.E., 1999, GRL, **26**, 627

Cargill, P. J., Chen, J., Spicer, D. S. and Zalesak, S. T., 1996, JGR, **101**, 4855

Castelli, J.P., Aarons, D.A., and Michael, G.A. 1967, JGR, **72**, 5491

Chen, J., 1989, ApJ, **338**, 453

Chen, J., 1996, JGR, **101**, 27499

Chen, J. 1997, Geophysical Monograph, **99**, 65

Chen, J. and 9 others, 1997, Ap.J. Letters, **490**, L191

Chen, J., Santoro, R. A., Krall, J., Howard, R. A., Duffin, R., Moses, J. D., Brueckner, G. E., Darnell, J. A. and Burkepile, J. T., 2000, ApJ, **533**, 481

Cliver, E.W., McNamara, L.F. and Gentile, L.C. 1985, JGR, **90**, 6251

Cliver, E.W., Webb, D.F. and Howard, R.A. 1998, Solar Phys. **107**, 89

Falconer, D. A., Gary, G. A., Moore, R. L. and Porter, J. G., 2000, Ap.J., **528**, 1004

Feldman, U., 1998, Space Sci. Rev. **85**, 227

Feynman, J. and Martin, S.F., 1995, JGR, **100**, 3355

Forbes, T.G., 2000, Adv., Space Rev., **26**, 549

Forbush, S.E., 1946, Phys. Rev. **70**, 771

Gloeckler, G., et al., 1994 JGR, **99**, 17,637

Gloeckler, G. et al., 1999, GRL **26**, 157

Gopalswamy, N. et al. 1998, JGR **103**, 307

Gopalswamy, N., Lara, A. & Kaiser, M.L. 2000, Bulletin AAS, **32**, 0283

Gosling, J.T., 1990, GMS, **58**, 343

Hagyard, M. J., Smith, J. B., Jr., Teuber, D. and West, E. A., 1984, Solar Physics, **91**, 115

Hagyard, M. J., Venkatakrishnan, P. and Smith, J. B., Jr., 1990, Ap.J. Suppl, **73**, 159

Harrison, R.A., 1993, Advanced Space Review, **14**, 23

Harrison, R.A., 1995, Astron. and Astrophys., **304**, 585

Huba, J.D. and Chen, J., 1996, ApJ, **469**, 412

Kahler, S. W., Sheeley, N. R., Jr., Howard, R. A., Michels, D. J., Koomen, M. J., McGuire, R. E., von Rosenvinge, T. T. and Reames, D. V., 1984, JGR, **89**, 9683

Klimas, A.J., Vassiliadis, D., Baker, D.N. 1997, JGR, **102**, 26993

Klimas, A.J., Vassiliadis, D., Baker, D.N. 1998, JGR, **103**, 20435

Klimchuk, J.A. 2000, Solar Physics, **193**, 53

Krall, J., Chen, J., Santoro, R., Spicer, D. S., Zalesak, S. T., and Cargill, P. J., 1998, ApJ,**500**, 992

Krall, J., Chen, J. and Santoro, R., 2000, ApJ, **539**, 964

Kundu, M.R. and Haddock, F.T. 1960, Nature, **186**, 610

Kundu, M.R. and Stone, R.G. 1984, Adv. Sp. Res. **4**, 261

Lanzerotti, L. J., 1968, Phys.Rev.Lett., **21**, 929

Lanzerotti, L.J. , 1969, J. Spacecraft and Rockets, **6**, 1086

Lanzerotti, L.J., Krimigis, S.M., Decker, R.B., Hawkins III, S.E., Gold, R.E., Armstrong, T.P., and Roelof, E.C., 2000, Space Sci. Rev. in press

Lee, M.A. 2000, Proc. ACE 2000 Symposium, (R.A. Mewaldt et al., eds.), AIP CP528, 3

Lee, M.A. and Ryan, J.M., 1986, ApJ Letters, **303**, L829

Leka, K.D., Canfield, R.C., McClymont, A.N., Delabeau-jaudiere, J.F., Fan, Y.H., and Tang, F., 1993, Ap.J., **411**, 370

Li, W., Lee, C.Y., Chae, J., Wang, J., Goode, P.R., Wang, H. and Ai, G., 2000, Ap.J., submitted

Malitson, H.H., Fainberg, J. and Stone, R.G., 1973, Astrophys. Lett. **14**, 111

Marubashi, K., 1997, in "Coronal Mass Ejections", Eds., Crooker, Joselyn and Feynman, Geophysical Monograph **99**, p147

O'Brien, T. P. and R. L. McPherron 2000, JGR **105**, 7707

Neidig, D., Wiborg, P., Confer, M., Haas, B., Dunn, R., Balasubramaniam, K.S., Gullixson, C., Craig, D., Kaufman, M., Hull, W., McGraw, R., Henry, T., Rentschler, R., Keller, K., Jones, H., Coulter, R., Gregory, S., Schimming, R. and Smaga, B. 1998, PASP Conf. Ser., **140**, 519

Neidig, D. F., Wiborg, P. H. Seagraves, J. Hirman, W. and Flowers, W.E. 1981, "An Objective Method for Forecasting Solar Flares," AFGL-TR-81-0026, Air Force Geophysics Laboratory (now AFRL), Hanscom AFB, MA

Ng, C.K. and Reames, D.V. 1994, ApJ, **424**, 1032

Reames, D.V., Barbier, L.M. and Ng, C.K. 1996, ApJ, **466**, 473

Reames, D.V. 1999, Space Sci. Rev. **90**, 413

Reiner, M.J., Kaiser, M.L., Fainberg, J. and Stone, R.G. 1998, JGR, **103**, 29651

Reiner, M.J., and Kaiser, M.L. 1999, GRL, **26**, 397

Reiner,0M.J., Kaiser, M.L., Plunkett, S.P., Prestage, N.P., and Manning, R. 20 0*a* ApJ Letters, **529**, L53

Reiner, M. J., Karlicky, M., Jiricka, K., Aurass, H., Mann, G., and Kaiser, M.L. 2000*b*, ApJ, **530**, 1049

Roach, P.J., 1998, in Fundamentals of Computational Fluid Dynamics, Hermosa, Albuquerque, N.M.

Shea, M.A. and Smart, D.F 1998 Adv. Space Res. **22**, 29

Smith, J.B., Neidig, D.F., Wiborg, P.H., West, E.A., Hagyard, M.J., Adams, M., Seagraves, P.H. 1996, PASP Conf. Ser., **95**, 55

Stone, R. ., et al., 1992, Astron. Astrophys. Suppl. Ser. **92**, 291

Tang, F. and Wang, H., 1993, Solar Physics, **143**, 107

Varsik, J. R., 1995, Solar Physics, **161**, 207

Wang, H., 1992, Solar Physics, **140**, 85

Wang, H., Zirin, H., Patterson, A., Ai, G. and Zhang, H., 1989, Ap.J., **343**, 489

Wang, H. Ewell, M. W., Jr., Zirin, H. and Ai, G., 1994, ApJ, **424**, 436

Wagner, W.J. and MacQueen, R.M. 1983, A&A, **120**, 136

Webb, D. F., Cliver, E. W., Crooker, N. U., St. Cry, O. C. and Thompson, B. J., 2000, JGR, **105**, 7491

White, S.M., Thomas, R.J., Brosius, J.W. and Kundu, M.R. 2000, ApJ, **534**, L203

Wild, J. P., 1950, Aust. J. Sci. Res. **A3**, 399

Wilson, R.M. and Hildner, E., 1984, Solar Physics, **91**, 169

Wilson, R.M. and Hildner, E., 1986, JGR, **91**, 5867

Wood, B. E., Karovska, M., Chen, J., Brueckner, G. E., Cook, J. W. and Howard, R. A., 1999, ApJ, **512**, 484

Wu, S.T. and Guo, W.P., 1997, Adv. Space Rev., **20**, 2313

Wu, S.T., Guo, W.P. and Dryer, M., 1997a, Solar Physics, **170**, 265

Wu, S.T. and 17 others, 1997b, Solar Physics, **175**, 719

Wu, S.T. and 14 others, 1997c, ESA SP-404, 739

Wu, S.T. and Guo, W.P., 1997d, Geophys. Monogram, **99**, 83

Wu, S.T., Guo, W,P., Michels, D.J. and Burlaga, L., 1999, JGR, **104**, 14789

Wu, S.T., Wang, A.H., Plunkett, S.P. and Michols, D.J., 2000, Ap. J., in press

Zurbuchen, T. H., G. Gloeckler, et al., 2000, *Sources of the solar wind during solar activity maximum,* JGR, in press

Zurbuchen, T. H., et al., 1998, Space Sci. Rev., **85**, 397